NASA Contractor Report 145110

(NASA-CR-145110) ACOUSTOELASTICITY (Princeton Univ., N. J.) 99 p HC A05/MF A01 CSCL 20A

N77-28908

Unclas

G3/71 40720

ACOUSTOELASTICITY.

E. H. DOWELL

PRINCETON UNIVERSITY

GRANT NSG-1253

July 1977

AUG 1977
RECEIVED
NASA STI FACILITY
INPUT BRANCH

National Aeronautics and
Space Administration

Langley Research Center
Hampton, Virginia 23665

ACOUSTOELASTICITY

E. H. Dowell
Princeton University

		Page
I	INTRODUCTION	1
II	HELMHOLTZ RESONATOR	2
III	COUPLED FLUID-STRUCTURAL MOTION OF AN ACOUSTIC CAVITY WITH A FLEXIBLE AND/OR ABSORBING WALL	7
IV	A VARIATIONAL FORMULATION	17
V	ACOUSTIC NATURAL MODES IN MULTIPLY CONNECTED CAVITIES	24
VI	FORCED RESPONSE OF A CAVITY WITH A FLEXIBLE AND/OR ABSORBING WALL	31
VII	NUMERICAL RESULTS AND COMPARISONS WITH EXPERIMENT	46
VIII	CONCLUDING REMARKS	58
	REFERENCES	60
	APPENDIX A ACOUSTIC NORMAL MODES OF A CAVITY WITH RIGID WALLS	63
	APPENDIX B STANDING WAVES IN MULTIPLY CONNECTED CAVITIES USING A GREEN'S FUNCTION APPROACH	68
	FIGURES	71

LIST OF SYMBOLS

A	- wall area
a	- cavity length; panel length
a_n	- velocity potential generalized coordinate; see equation III-26
b	- cavity width; panel width
C_{nr}	- see equation III-8$_A$
c_o	- ambient (equilibrium) speed of sound
d	- cavity depth
F_n	- n^{th} acoustic natural mode
I_A	- acoustic action integral
I_p	- plate action integral
L_{nm}	- see equation III-14
ℓ	- neck length of Helmholtz resonator
M_n^A	- n^{th} acoustic generalized mass; see equation III-5
m	- structural mass/area
n	- normal to surface
P_n	- n^{th} acoustic modal pressure; see equation III-7
p	- pressure
Q_n	- m^{th} wall generalized force; see equation III-12
q_m	- m^{th} wall modal coordinate; see equation III-11
M_m	- n^{th} structural generalized mass; see equation III-18
T_A	- acoustic kinetic energy
T_p	- kinetic energy of plate
t	- time

$\vec{u}$ - fluid particle displacement vector

V_A - acoustic potential energy

V_p - strain energy of plate

V - volume

W - work

W - wall amplitude

W_n - n^{th} acoustic mode wall deflection; see equation III-7

w - wall deflection

x,y,z - cartesian coordinates

z - impedance

ξ - displacement of fluid

ϕ - velocity potential

γ - ratio of specific heats

λ - see equation VI-33

ψ_m - m^{th} (structural) wall natural mode

ρ - density

ζ_m - m^{th} structural mode (critical) damping ratio

$\zeta_n{}^c$ - n^{th} acoustic cavity mode (critical) damping ratio

ω - frequency

$\Omega_m{}^E, \Omega_m{}^A$ - see equation VI-33

Subscripts

o - equilibrium

- perturbation

A - absorbent wall; acoustic

F - flexible wall

H - Helmholtz resonator

m,n,r,s - modal numbers

R - rigid wall

Superscripts

A - acoustic

a,b,c - cavity a,b,c, respectively

E - external

c - acoustic cavity

* - complementary

ORIGINAL PAGE IS
OF POOR QUALITY

METRIC CONVERSION FACTORS

Approximate Conversions to Metric Measures

Symbol	When You Know	Multiply by	To Find	Symbol
	LENGTH			
in	inches	*2.5	centimeters	cm
ft	feet	30	centimeters	cm
yd	yards	0.9	meters	m
mi	miles	1.6	kilometers	km
	AREA			
in^2	square inches	6.5	square centimeters	cm^2
ft^2	square feet	0.09	square meters	m^2
yd^2	square yards	0.8	square meters	m^2
mi^2	square miles	2.6	square kilometers	km^2
	acres	0.4	hectares	ha
	MASS (weight)			
oz	ounces	28	grams	g
lb	pounds	0.45	kilograms	kg
	short tons (2000 lb)	0.9	tonnes	t
	VOLUME			
tsp	teaspoons	5	milliliters	ml
Tbsp	tablespoons	15	milliliters	ml
fl oz	fluid ounces	30	milliliters	ml
c	cups	0.24	liters	l
pt	pints	0.47	liters	l
qt	quarts	0.95	liters	l
gal	gallons	3.8	liters	l
ft^3	cubic feet	0.03	cubic meters	m^3
yd^3	cubic yards	0.76	cubic meters	m^3
	TEMPERATURE (exact)			
°F	Fahrenheit temperature	5/9 (after subtracting 32)	Celsius temperature	°C

*1 in = 2.54 (exactly)

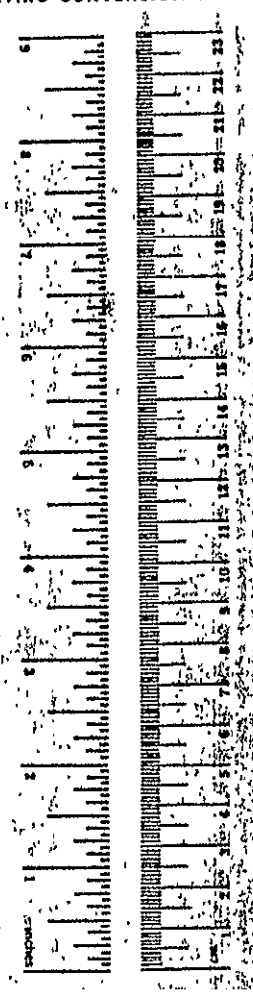

Approximate Conversions from Metric Measures

Symbol	When You Know	Multiply by	To Find	Symbol
	LENGTH			
mm	millimeters	0.04	inches	in
cm	centimeters	0.4	inches	in
m	meters	3.3	feet	ft
m	meters	1.1	yards	yd
km	kilometers	0.6	miles	mi
	AREA			
cm^2	square centimeters	0.16	square inches	in^2
m^2	square meters	1.2	square yards	yd^2
km^2	square kilometers	0.4	square miles	mi^2
ha	hectares (10,000 m^2)	2.5	acres	
	MASS (weight)			
g	grams	0.035	ounces	oz
kg	kilograms	2.2	pounds	lb
t	tonnes (1000 kg)	1.1	short tons	
	VOLUME			
ml	milliliters	0.03	fluid ounces	fl oz
l	liters	2.1	pints	pt
l	liters	1.06	quarts	qt
l	liters	0.26	gallons	gal
m^3	cubic meters	35	cubic feet	ft^3
m^3	cubic meters	1.3	cubic yards	yd^3
	TEMPERATURE (exact)			
°C	Celsius temperature	9/5 (then add 32)	Fahrenheit temperature	°F

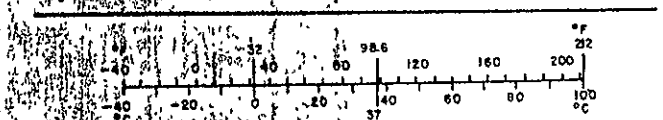

I INTRODUCTION

We consider internal sound fields, i.e. sound or pressure variations inside of bounded enclosures. We proceed from the simplest geometry to the more complex. Specifically the interaction between the (acoustic) sound pressure field and the (elastic) flexible wall of an enclosure will be considered. One might think of this as the field of "acoustoelasticity". A good introduction to this subject is given in "Sound, Structures and their Interaction" by Junger and Feit[1]. Also the author has briefly discussed this subject in his book, "Aeroelasticity of Plates and Shells"[2].

From the point of view of applications, such problems frequently arise when the vibrating walls of a transportation vehicle induce a significant internal sound field. The walls themselves may be excited by external fluid flows. Cabin noise in various flight vehicles and the internal sound field in an automobile are representative examples.

The first physical model to be considered is a simple one; but one which is famous in the acoustic literature.

II HELMHOLTZ RESONATOR

The reader may also wish to consult Kinsler & Frey, Fundamentals of Acoustics, pp. 187-207, on this topic.[3]

Consider a "small" volume (any linear dimension small compared to the acoustic wavelength) so that we may consider all properties constant within the volume. For example, consider a box with one vibrating wall

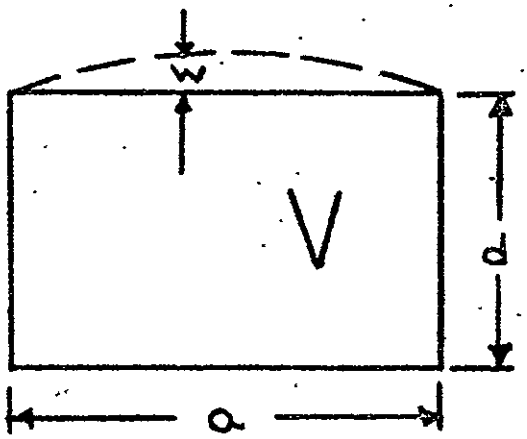

We wish to relate the wall motion to the cavity pressure change and compute the coupled structural-acoustic natural frequency.

From the isentropic gas law

$$p = k \quad \rho^{\gamma} \tag{1}$$

and conservation of mass

$$\rho V = \text{constant} \tag{2}$$

Consider small changes denoted by $(\hat{\ })$ from an equilibrium condition denoted by $()_0$.

$$\rho = \rho_o + \hat{\rho}$$

$$p = p_o + \hat{p}$$

$$V = V_o + \hat{V} \tag{3}$$

Substituting (3) into (1) and (2), and linearizing in ($\tilde{}$),

$$\frac{\hat{p}}{p_o} = \gamma \frac{\hat{\rho}}{\rho_o} \tag{4}$$

$$\frac{\hat{\rho}}{\rho_o} + \frac{\hat{V}}{V_o} = 0 \tag{5}$$

Combining (3) and (4)

$$\frac{\hat{p}}{p_o} = -\gamma \frac{\hat{V}}{V_o} \tag{6}$$

Now

$V_o = Ad$ where A is wall area

$\hat{V} = \iint wdxdy$

Thus

$$\frac{\hat{p}}{p_o} = -\gamma \frac{\iint wdxdy}{Ad} \tag{7}$$

This is essentially the "Helmholtz resonator" approximation. The equation of motion of the wall is thus

$$m \frac{\partial^2 w}{\partial t^2} = -\frac{\gamma p_o}{Ad} \iint wdxdy \tag{8}$$

We have ignored the stiffness of the wall (which is valid for large acoustical stiffness, e.g., small depths) and also ignored acoustical inertia (which is valid for low frequencies, e.g., large wavelengths).

One can approximately solve (8) using Galerkin's method.

Assume

$$w = W \sin \frac{\pi x}{a} \sin \frac{\pi y}{b} \tag{9}$$

$$A = ab$$

Substitute above into (8), multiply by $\sin \frac{\pi x}{a} \sin \frac{\pi y}{b}$ and integrate over the plate area. The result is

$$m \frac{d^2W}{dt^2} + \gamma p_o \frac{W}{d} \frac{64}{\pi^4} = 0 \tag{10}$$

Substituting $W = \overline{W} e^{i\omega t}$, we may compute the natural frequency as

$$\omega^2 = \frac{\gamma p_o}{md} \frac{64}{\pi^4} \tag{11}$$

Now the problem we have just analyzed is <u>not</u> the one that Helmholtz analyzed. Helmholtz considered a bottle with a neck as in the followings sketch:

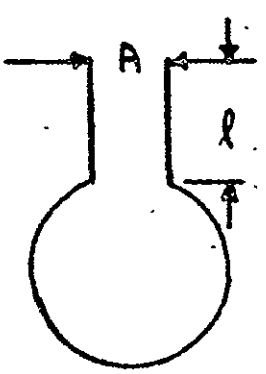

Denote by ξ the displacement of the fluid in the neck of the bottle. <u>This</u> fluid is considered incompressible and is treated as a rigid body. The equation of motion is

$$\rho_o A\ell \frac{d^2\xi}{dt^2} = \left[-\gamma p_o \frac{A\xi}{V_o}\right] A \tag{12}$$

The natural frequency is

$$\omega^2 = \frac{\gamma p_o A}{V_o \rho_o \ell} \tag{13}$$

$$= \frac{c_o^2 A}{V_o \ell}$$

It is this problem which is usually termed the "Helmholtz resonator".

One can also consider the problem of an applied external pressure, p^E, acting on the neck. The equation of motion is

$$\rho_o \ell \frac{d^2\xi}{dt^2} = - \frac{\gamma p_o A}{V_o} \xi + p^E \tag{14}$$

For the particular case of simple harmonic motion where

$$p^E = \bar{p}^E e^{i\omega t}$$

$$\xi = \bar{\xi} e^{i\omega t}$$

one may obtain from (14),

$$\frac{\bar{p}^E}{\bar{\xi}} = \frac{-\rho_o \ell \omega^2 + \frac{\gamma p_o A}{V_o}}{1}$$

Thus an "impedance" may be defined as

$$z_H \equiv \frac{\overline{p}^E}{i\omega\overline{\xi}} = \rho_o \ell \, i\omega + \frac{\gamma \, p_o A}{V_o \, i\omega} \tag{15}$$

where $i\omega\overline{\xi} \equiv$ velocity amplitude and z_H is the impedance of the Helmholtz resonator.

The internal cavity pressure, p^c, can be computed from the above for a sinusoidal external pressure as

$$\frac{\overline{p}^c}{\overline{p}^E} = \frac{1}{\dfrac{\rho_0 \ell \omega^2 V}{\gamma p_0 A} - 1} \tag{16}$$

$$\text{or} = \frac{1}{\dfrac{\ell V}{A} \dfrac{\omega^2}{c_0^{\,2}} - 1}$$

A similar expression can be obtained for the membrane example first considered. The significance of (16) for our purposes is that it shows that for

$$\frac{\ell V}{A} \cdot \frac{\omega^2}{c_0^{\,2}} < 2 \quad \text{then} \quad \left| \frac{\overline{p}^c}{\overline{p}^E} \right| > 1$$

Hence for low frequency excitations the internal cavity pressure will exceed the external pressure level.

It is emphasized that the perturbation pressure is assumed not to vary within the volume in this model. This is reasonable so long as the acoustic wavelength, $\lambda = \frac{c_o \, 2\pi}{\omega}$, is much larger than any characteristic dimension of the volume. Also the fluid properties are assumed not to vary within the neck.

III COUPLED FLUID-STRUCTURAL MOTION OF AN ACOUSTIC CAVITY WITH A FLEXIBLE AND/OR ABSORBING WALL.

We consider again the enclosed volume which was considered in connection with the Helmholtz resonator problem.

A direct and concise derivation of the acoustic pressure in a closed cavity due to arbitrary motion of the flexible cavity walls will be given. The pressure is expanded in terms of the normal modes of the rigid-walled cavity. The result, which is valid for any cavity geometry, is given in the form of a set of linear ordinary differential equations for the response of each normal mode. For the sake of completeness the equations of motion of the flexible wall are also derived in terms of structural normal modes and hence the complete coupled fluid-structural equations of motion are given.

Most studies of the acoustic pressure within a cavity due to motion of a flexible wall have considered <u>only simple harmonic motion</u>,[4,5,6] although implicitly the more general case of arbitrary motion can be handled via the Fourier integral theorem. However, a very simple result for <u>arbitrary wall motions</u> can be obtained directly from the acoustic equations using Green's Theorem without resorting to transform methods. The end result of the present method is an expansion for the acoustic pressure within the cavity due to motion of the walls, in terms of the normal modes of the cavity with its walls assumed to be rigid. The derivation applies equally to all cavity geometries, and as such is a generalization of the normal mode expansion (or "guided wave" expansion,

in the terminology used there) derived less directly and for rectangular cavities only in [7].

Acoustical Problem

Let the cavity occupy a volume V, and be surrounded by a wall surface A, of which the portion A_F is flexible, while the remainder A_R is rigid. If the fluid within the cavity is at rest prior to motion of the wall, the fluid pressure p^* satisfies the familiar wave equation, and associated boundary condition:

$$\nabla^2 p - \frac{1}{c_o^2}\frac{\partial^2 p}{\partial t^2} = 0 \tag{1}$$

$$\begin{aligned} \frac{\partial p}{\partial n} &= -\rho_o \frac{\partial^2 w}{\partial t^2} \quad \text{on } A_F \\ &= 0 \qquad\qquad \text{on } A_R \end{aligned} \tag{2}$$

In these equations ρ and c are the equilibrium fluid density and acoustic velocity within the cavity, and w is the displacement of the flexible portion of the wall in the normal direction n (positive outward).

Equation (1) has normal mode solutions $F_n e^{i\omega t}$, n = 0,1,2,... with the following properties

$$\nabla^2 F_n = -\left(\frac{\omega_n}{c_o}\right)^2 F_n \tag{3}$$

$$\frac{\partial F_n}{\partial n} = 0 \quad \text{on } A \tag{4}$$

*This is the perturbation pressure $\hat{p}$, of course. The ^ is dropped subsequently for convenience.

$$\frac{1}{V}\int_V F_r F_n dv = 0 \qquad r \neq n \tag{5}$$

$$\equiv M_n^A \qquad r = n$$

ω_n^A is the nth acoustical natural frequency and F_n its related natural mode. Superscript A is to distinguish ω_n^A and M_n^A from their structural counterparts to be discussed in a later section.

Note that equation (3) has the solution $\omega_0^A = 0$, $F_0 = 1$. All other frequencies ω_n^A, $n = 1,2,\ldots$ are positive and non-zero, however. A brief review of acoustical normal mode theory is given in Appendix A.

The wave equation (1) can be transformed into a set of ordinary differential equations in time by using Green's Theorem in the form:

$$\int_V (p\nabla^2 F_n - F_n \nabla^2 p) dv = \int_A \left(p\frac{\partial F_n}{\partial n} - F_n \frac{\partial p}{\partial n}\right) dA \tag{6}$$

By defining

$$P_n \equiv \frac{1}{\rho_0 c_0^2 V} \int_V p F_n dv$$

$$W_n \equiv \frac{1}{A_F} \int_{A_F} w F_n dA \tag{7}$$

and making use of the fact that p and F_m satisfy equations (1) and (3), and boundary conditions (2) and (4), the following ordinary differential equations for the acoustic modes are obtained from (6):

$$\ddot{P}_n + \omega_n^{A2} P_n = - \ddot{W}_n \frac{A_F}{V} \qquad (8)^*$$

A dot (˙) denotes differentiation with respect to time. The quantities $P_m(t)$ are the coefficients in an acoustical normal mode expansion for the pressure:

$$P \equiv \frac{p}{\rho_0 c_0^2} = \sum_n \frac{P_n}{M_n^A} F_n \qquad (9)^*$$

Since the normal modes F_n satisfy the homogeneous boundary condition (4) on the entire wall surface A, the normal derivative of expression (9) does not converge uniformly on the flexible portion A_F of the wall surface. Expression (9) is suitable, however, for calculating the pressure itself throughout the cavity and everywhere on the wall surface, including the flexible portion.

When one of the walls of the cavity is highly absorbent it is usual to model it through a simple point-impedance model where it is assumed that

$$p = z_A \dot{w}_A \quad \text{on } A_A \qquad (10)$$

where the A subscript is used to refer to the absorbent wall characteristics, e.g.

w_A - absorbent wall displacement

z_A - absorbent wall impedance.

*Note that for n = 0, we have the Helmholtz resonator result, i.e.

$$F_0 = 1$$

$$W_0 = \frac{\int w dA}{A_F} \qquad P_0 = - W_0 \frac{A_F}{V}$$

$$M_0^A = 1 \qquad \therefore p = \rho_0 c_0^2 P_0 = - \rho_0 c_0^2 \frac{\int w dA}{V}$$

The boundary condition

$$\frac{\partial p}{\partial n} = -\rho_0 \ddot{w}_A \qquad \text{on } A_A \tag{2}$$

still applies, of course. Using (10), (2) may be written for the absorbing wall as

$$\frac{\partial p}{\partial n} = -\rho_0 \dot{p}_{z_A} \qquad \text{on } A_A \tag{2_A}$$

Using the above in (6) along with (9), (8) becomes

$$\ddot{P}_n + \omega_n^{A^2} P_n + \frac{A_A}{V}\rho_0 c_0^2 \sum_r \dot{P}_r \frac{C_{nr}}{M_r^A} = -\frac{A_F}{V} \ddot{W}_n \tag{8_A}$$

where $C_{nr} \equiv \iint_{\text{over } A_A} \frac{F_n \frac{F_r}{z_a} dA}{A_A}$

The effect of an absorbent wall is to couple all of the (rigid wall) acoustic modes. Of course, as we will see explicitly in what follows, the flexible wall also couples all of the acoustic modes as well.

Structural Modal Expansion

In many technical applications the flexible portion A_F of the cavity wall may be a structural element, such as a plate or shell. In such cases the wall deflection w is often expressed as a series of the form

$$w = \sum_m q_m \Psi_m \tag{11}$$

in which the modal functions Ψ_m are defined over the region A_F, their properties being determined by structural considerations. Using (11) a set of structural modal equations describing the wall motion are derived. As will be shown subsequently, in these equations the cavity acoustic pressure, p, appears in the form of generalized forces Q_m:

$$Q_m \equiv \int_{A_F} \Psi_m p \, dA \tag{12}$$

First, however, the quantities W_m appearing in (8) and (8_A) can be expressed using (7) and (11) as

$$W_n = \sum_m L_{nm} q_m \tag{13}$$

where

$$L_{nm} \equiv \frac{1}{A_F} \int_{A_F} F_n \Psi_m \, dA \tag{14}$$

Hence, (8_A) becomes the acoustic modal equation

$$\ddot{P}_n + \omega_n^{A^2} P_n + \frac{A_A \rho_0 c_0^2}{V} \sum_r \dot{P}_r \frac{C_{nr}}{M_r^A} = - \sum_m \frac{A_F}{V} L_{nm} \ddot{q}_m \tag{15}$$

These can then be solved in conjunction with the companion structural equations to be derived in the next section.

Structural Considerations

When the structure may be represented by a linear structural model the total fluid-structural interaction may be treated in a simple way. Let the structure be represented by a linear (partial, differential) equation.

$$S\,w + m\,\frac{\partial^2 w}{\partial t^2} = p^c - p^E \tag{16}$$

S is a linear differential operator, representing structural stiffness. For example, for an isotropic, flat plate, $S \equiv D\nabla^4$, where ∇^4 is the biharmonic operator. The second term on the left-hand side is the structural inertia, m being structural mass per unit area. On the right-hand side we have two pressure loadings, the first due to the cavity acoustics, the second due to some specified "external" agent.

For simplicity, we assume that the structural modes, ψ_m, (cf.(11)) are normal structural modes satisfying an eigenvalue equation

$$S\psi_m - m\,\psi_m\,\omega_m^2 = 0 \tag{17}$$

and associated orthogonality condition

$$\int_{A_F} m\,\psi_m\psi_r\,dA \equiv M_m \qquad \text{for } m = r \tag{18}$$

$$= 0 \qquad \text{for } m \neq r$$

ω_m is the mth structural natural frequency and ψ_m its associated normal mode.

Substituting (11) into (16), using (17), gives

$$\sum_m m\,\left[\frac{d^2 q_m}{dt^2} + \omega_m^2\,q_m\right]\psi_m = p^c - p^E \tag{19}$$

Multiplying through by ψ_n and integrating over A_F gives, using (18),

$$\left[\frac{d^2 q_m}{dt^2} + \omega_m^2\,q_m\right] M_m = Q_m^c + Q_m^E \tag{20}$$

where (recall (12))

$$Q_m^c \equiv \int p^c\,\psi_m\,dA. \tag{21}$$

$$Q_m^E \equiv - \int p^E \psi_m \, dA \tag{22}$$

From (9) and (21),

$$Q_m^c = A_F \rho_0 c_0^2 \sum_n P_n \frac{L_{nm}}{M_n^A} \tag{23}$$

Hence the structural modal equations, (20), may be rewritten using (23) as

$$M_m[\ddot{q}_m + \omega_m^2 \; q_m] = \rho_0 c_0^2 A_F \sum_n P_n \frac{L_{nm}}{M_n^A} + Q_m^E \tag{24}$$

Summarizing the key relations are (15) and (24) with Q_n^E determined from its definition, (22). (15) and (24) are coupled acoustical-structural ordinary differential equations which may be solved by any standard method. Since we normally are dealing with systems under forced motion, Q_n^E, the initial conditions on q_m and P_n will usually be the trivial ones.

$$q_m = \frac{dq_m}{dt} = P_n = \frac{dP_n}{dt} = 0 \quad \text{at } t = 0$$

Of course, any physically meaningful initial conditions, could be accommodated.

It should be noted that in applications, the use of normal structural modes may not always be convenient and hence direct structural coupling may occur. Of course, this will always be true for a nonlinear structural model [7] since the concept of normal modes loses much of its significance there.

Finally, although the acoustic pressure is obviously the physical variable of the greatest interest, some additional insight into the nature of the structural-acoustic interaction can be obtained by

considering instead the acoustic velocity potential. The two are related through Bernouilli's equation

$$p = -\rho_0 \dot{\phi} \tag{25}$$

If ϕ is expanded in its natural modes (they are obviously the same modes as for p from the above)

$$\phi = \Sigma a_n F_n \tag{26}$$

one can from (9), recall

$$p = \rho_0 c_0^2 \sum_n \frac{P_n F_n}{M_n^A} \tag{9}$$

(25) and (26), determine that

$$c_0^2 \frac{P_n}{M_n^A} = -\dot{a}_n \tag{27}$$

Using (27) in (15) and (24), one obtains

$$VM_n^A [\ddot{a}_n + \omega_n^{A^2} a_n]$$

$$+ A_A \rho_0 c_0^2 \sum_r \dot{a}_r C_{nr} = \underline{c_0^2 A_F \sum_m L_{nm} \dot{q}_m} \tag{15*}$$

$$M_m [\ddot{q}_m + \omega_m^2 q_m] = \underline{-\rho_0 A_F \sum_n \dot{a}_n L_{nm}} + Q_m^E \tag{24*}$$

The underlined terms are the structural-acoustic coupling terms. The coefficients are anti-symmetric (to within a multiplicative constant) and this characteristic, combined with the first time derivatives of

q_m and a_n, means that the equations possess gyroscopic coupling. Thus it is known that (if $A_A \to 0$ so that there is no absorbing wall) the coupled structural - acoustic natural frequencies are real, i.e. the system without absorbing walls is an undamped resonator. Moreover Meirovitch[8] (in a different physical context) has shown how one may use conventional matrix eigenvalue methods to determine the natural frequencies of gyroscopically coupled systems.

IV A VARIATIONAL FORMULATION

The same results may be obtained through a variational formulation. Previously Gladwell[9-11] and later Craggs[12-13] have considered variational statements in the context of finite element representations for the coupled structural (wall) - acoustic (cavity) problem. Craggs' work has been carried furthest and we use it as a point of departure for our discussion. Even though we shall obtain the same results as before, the variational statement in its present form is somewhat awkward. Hence the author's preference is for the previous formulation using Green's theorem for the cavity. Others may feel differently, however, or perhaps be inspired to develop a more elegant and/or simpler variational statement. Hence the following brief discussion. Following Craggs, consider an action integral for the plate

$$I_p \equiv \int_{t_1}^{t_2} [T_p - V_p + (W_E - W_A)]\, dt \tag{28}$$

where

$$T_p = 1/2 \iint m \left(\frac{\partial w}{\partial t}\right)^2 dxdy$$ Plate Kinetic Energy of Flexible Wall

$$V_p = \frac{D}{2} \iint \left[\left(\frac{\partial^2 w}{\partial x^2}\right)^2 + \left(\frac{\partial^2 w}{\partial y^2}\right)^2 + 2\nu \frac{\partial^2 w}{\partial x^2}\frac{\partial^2 w}{\partial y^2} + 2(1-\nu)\left(\frac{\partial^2 w}{\partial x \partial y}\right)^2\right] dxdy$$

Strain Energy of Wall

$$\delta W^E = - \iint p^E\, \delta w\, dxdy$$ Virtual work due to External pressure

$$\delta W^A = \iint p^c\, \delta w\, dxdy \tag{29}$$

or

$$\delta W^A = - \iint \rho_0 \dot{\phi}\, \delta w\, dxdy$$ Virtual work due to Acoustic Cavity pressure

Bernoulli's relation has been used to obtain the last line, i.e.

$$p^c = - \rho_0 \dot{\phi}$$

Using Hamilton's Principle on I_p (with p^E and p^c not varied) one obtains

$$m\ddot{w} + D\nabla^4 w = -p^E + p^c \tag{30}$$

with appropriate boundary conditions on the plate edges involving w and its derivatives.

The action integral for the acoustic system with a prescribed motion at the cavity surface is

$$I_A \equiv \int_{t_1}^{t_2} (T_A - V_A - W^*_A)dt \tag{31}$$

where $\vec{u}$ - (vector) particle fluid displacement

$$T_A = 1/2 \iiint \rho_0 \dot{\vec{u}} \cdot \dot{\vec{u}}\, dxdydz \qquad \text{Acoustic Kinetic Engery}$$

$$V_A = 1/2 \iiint \frac{p^2}{\rho_0 c_0^2}\, dxdydz \qquad \text{Acoustic Potential Energy} \tag{32}$$

$$\delta W^*_A = \iint w\, \delta p\, dxdy$$

δW^*_A is the complementary work done by the virtual forces (acting through the real displacements) at the structural-acoustic interface. Introducing the velocity potential, ϕ,

$$\dot{\vec{u}} = \nabla\phi$$

and recalling Bernoulli's relation

$$p^c = -\rho_0\dot{\phi}$$

the above may be written as

$$T_A = 1/2 \iiint \rho_0 (\nabla\phi \cdot \nabla\phi) dxdydz$$

$$V_A = 1/2 \iiint \frac{\rho_0}{c_0^2}(\dot{\phi})^2 \, dxdydz \tag{33}$$

$$\delta W^*_A = - \iint w \, \rho_0 \delta \dot{\phi} \, dxdy$$

Using Hamilton's Principle with respect to I_A (with w <u>not</u> varied) one obtains

$$\nabla^2 \phi - 1/_{c_0^2} \ddot{\phi} = 0 \tag{34}$$

with the boundary condition

$$\frac{\partial \phi}{\partial z} = \dot{w} \tag{35}$$

on $z = 0$ (flexible wall)

As the attentive reader will already have noted, our use of cartesian coordinates is a matter of convenience and the results readily carry over to cavities and flexible walls of arbitrary shape.

The necessity for considering both virtual work, δW_A, and complementary virtual $\delta W_A{}^*$ makes this variational statement appear somewhat cumbersome to the author and it is for this reason that the earlier approach using Green's Theorem is preferred.

It is worth noting that an absorbing wall in the cavity can also be included, specifically in δW^*_A. We add a subscript, A, to all quantities to denote absorbent. The complementary virtual work due to the absorbing wall is

$$\delta W^*_{AA} = - \iint w_A \, \rho_0 \delta \dot{\phi} dxdy$$

Realizing that in Hamilton's Principle the above will appear as

$$\int_{t_1}^{t_2} \delta W^*_{AA}\, dt$$

one may integrate by parts to obtain

$$\int_{t_1}^{t_2} \delta W^*_{AA}\, dt = \iiint \dot{w}_A\, \rho_0 \delta\phi\, dxdy\, dt$$

Further if we model the absorbing wall through a simple point-impedance model then

$$\bar{p} = z_A\, \dot{w}_A \tag{36}$$

or

$$-\rho_0 \dot{\phi} = z_A\, \dot{w}_A \quad \text{on } A_A$$

where z_A - absorbent wall impedance

Thus $\int_{t_1}^{t_2} \delta W^*_{AA}\, dt = -\iiint \frac{\rho_0^2}{z_A} \dot{\phi}\, \delta\phi\, dxdy\, dt$

Using the above and proceeding through the formalism of Hamilton's Principle one obtains for the boundary condition on the absorbing surface (e.g. say $z = d$)

$$\frac{\partial\phi}{\partial z} = \dot{w}_A$$

or

$$\frac{\partial\phi}{\partial z} = -\frac{\rho_0^2}{z_A} \quad \text{on } z = d \tag{37}$$

Modal Equations

Modal expansions are now made for w and ϕ.

$$w = \Sigma\, q_m(t)\ \psi_m(x,y)$$

$$\phi = \Sigma\, a_n(t)\ F_n(x,y,z)$$

It is simplest conceptually and generally most efficient computationally to choose the in vacuuo plate modes for ψ_m and the rigid wall modes for F_m. Other possibilities exist, of course, but they shall not be pursued here. Using the above choice, one has

$$T_p = 1/2 \sum_m M_m\ \dot{q}_m^{\,2}$$

$$V_p = 1/2 \sum_m M_m\ \omega_m^{\,2}\ q_m^2 \tag{38}$$

where $M_m \equiv \iint m\ \psi_m^{\,2} dxdy$ generalized plate mass

ω_m - m^{th} in vacuuo natural plate frequency

Here we have used the orthogonality of the ψ_m, i.e.

$$\iint m\ \psi_m\ \psi_n\ dxdy = 0 \quad \text{for } \omega_m \neq \omega_n$$

Also to obtain V_p an integration by parts has been used along with the fact that ψ_m, ω_m satisfy the Euler-Lagrange equation

$$D\nabla^4\ \psi_m - \omega_m^{\,2}\ m\ \psi_m = 0$$

and appropriate boundary equations for ψ_m on the plate edges.

One also has

$$\delta W_E = \Sigma\ Q_m^{\,E}\ \delta q_m \tag{39}$$

where

$$Q^E_m \equiv -\int p^E\ \psi_m\ dxdy$$

and $\delta W_A = - A_F \rho \sum_n \sum_m \dot{a}_n \delta q_m L_{nm}$

where $L_{nm} \equiv \dfrac{\iint_{\text{over } A_F} F_n \psi_m \, dxdy}{A_F}$ (40)

$A_F \equiv$ total area of (flexible) structural wall.

Using Hamilton's Principle one obtains, in the usual way, the structural modal equations

$$-M_m[\ddot{q}_m + \omega_m{}^2 q_m] + Q_m{}^E - A_F \rho_0 \sum_n \dot{a}_n L_{nm} = 0 \tag{41}$$

Turning now to the determination of the acoustic modal equations, one may construct

$$T_A = 1/2 \, V \frac{\rho_0}{c_0^2} \sum_n \omega_n^{A^2} M_n^A a_n^2$$

$$V_A = 1/2 \, V \frac{\rho_0}{c_0^2} \sum_n M_n{}^A \dot{a}_n^2 \tag{42}$$

where

$$M_n{}^A \equiv \frac{\iiint F_m{}^2 \, dxdydz}{V}$$

and $V \equiv$ total cavity volume, $\omega_n{}^A$ - n^{th} natural (rigid wall) cavity frequency

and $\delta W^*{}_A = - \rho_0 A_F \sum_m \sum_n q_m \delta \dot{a}_m L_{nm}$

$$\int_{t_1}^{t_2} \delta W^*{}_{AA} \, dt = - A_A \rho_0^2 \int \sum_n \sum_r \dot{a}_r \delta a_n C_{nr} dt$$

where $C_{nr} \equiv \frac{\iint_{\text{on } A_A} \frac{F_n F_r}{z_A} \, dxdy}{A_A}$

and $A_A \equiv$ total area of absorbing surface

In constructing T_A and V_A, we have used the orthogonality of F_m, i.e.

$$\iiint F_r \, F_n \, dxdydz = 0 \quad \text{for } \omega_n^A \neq \omega_r^A$$

and the fact that F_n, ω_n^A satisfy the Euler-Lagrange equation,

$$\nabla^2 F_n + \frac{\omega_n^{A^2}}{c_0^2} F_n = 0$$

and appropriate boundary conditions on the cavity walls.

Using Hamilton's Principle one obtains

$$VM_n^A \, [\ddot{a}_n + \omega_n^{A^2} \, a_n] - c_0^2 \, A_F \sum_m \dot{q}_m \, L_{nm} \tag{43}$$

$$+ \rho_0 c_0^2 \, A_A \sum_r \dot{a}_r \, C_{nr} = 0$$

Equations (41) and (43) are the same as equations (24)* and (15)* which were obtained previously.

V ACOUSTIC NATURAL MODES IN MULTIPLY CONNECTED CAVITIES

For definiteness we consider two rectangular cavities although it will be clear that the basic method is applicable to fairly general geometries. See sketch.

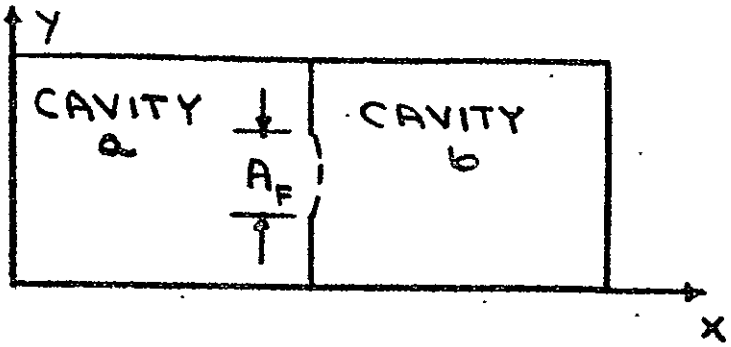

Our interest here is in the acoustic natural modes of the two cavities connected by an opening of area A_F. In this opening there is, in general, a flexible structural member which deforms (as indicated by the dashed line) and thus permits sound transmission from one cavity to the next. All other portions of the cavity walls are rigid. As before the structural member has a displacement, w, with a modal expansion

$$w = \sum_m q_m(t)\psi_m(y,z) \tag{1}$$

and the acoustical pressures in cavities a and b have modal expansions

$$p_a = \rho_0 c_0^2 \sum_n \frac{P_n^a F_n^a(x,y,z)}{M_n^{Aa}}$$

$$p_b = \rho_0 c_0^2 \sum_n \frac{P_n^b F_n^b(x,y,z)}{M_n^{Ab}} \tag{2}$$

The modal equations of motion for the acoustic pressures are then (recal Sections III and IV)

$$\ddot{p}_n^a + \omega_n^{Aa2}\, p_n^a = -\frac{A_F}{V_a} \sum_m \ddot{q}_m L_{nm}^a$$

$$\ddot{p}_n^b + \omega_n^{Ab2}\, p_n^b = +\frac{A_F}{V_b} \sum_m \ddot{q}_m L_{nm}^b \tag{3}$$

and for the structural wall

$$M_m[\ddot{q}_m + \omega_m^2\, q_m] = \rho_0 c_0^2 A_F \sum_n \frac{p_n^a L_{nm}^a}{M_n^{Aa}}$$

$$- \rho_0\, c_0^2 A_F \sum_n \frac{p_n^b L_{nm}^b}{M_n^{Ab}} \tag{4}$$

The + sign in the second of (3) and the - sign in the right hand side of (4) is a result of the normal to the opening being outward from cavity a and inward to cavity b.

As in Sections III and IV one may introduce a velocity potential through Bernoulli's equation

$$p^{a,b} = -\rho_0\, \dot{\phi}^{a,b} \tag{5}$$

with a modal expansion

$$\phi^{a,b} = \sum_n a_n^{a,b} F_n \tag{6}$$

(3) and (4) then become

$$V^a M_n^{Aa} [\ddot{a}_n^a + \omega_n^{Aa^2} a_n^a] = + c_0^2 A_F \sum_m L_{nm}^a \dot{q}_m$$

$$V^b M_n^{Ab} [\ddot{a}_n^b + \omega_n^{Ab^2} a_n^b] = - c_0^2 A_F \sum_m L_{nm}^b \dot{q}_m \tag{7}$$

and

$$M_m [\ddot{q}_m + \omega_m^2 q_m] = - \rho_0 A_F \sum_n \dot{a}_n^a L_{nm}^a$$

$$+ \rho_0 A_F \sum_n \dot{a}_n^b L_{nm}^b \tag{8}$$

(7) and (8) are in standard form for use of Meirovitch's algorithm[8] to determine the natural frequencies (eigenvalues) and modes (eigenvectors) of the two coupled cavities.

Of special interest is the case with a <u>pure</u> opening between the two cavities, i.e. one with zero mass and stiffness. In this case substantial further simplifications are possible. Thus $M_m = \omega_m = 0$ and (4) becomes (one could deal alternatively with (7) and (8))

$$\sum_n \frac{p_n^a L_{nm}^a}{M_n^{Aa}} - \sum_n \frac{p_n^b L_{nm}^b}{M_n^{Ab}} = 0 \tag{9}$$

To determine the natural frequencies, one assumes

$$q_m = \bar{q}_m e^{i\omega t}$$

$$p_n^{a,b} = \bar{p}_n^{a,b} e^{i\omega t} \tag{10}$$

Thus from (3) we may determine

$$\overline{P}_n^{a,b} = \mp \frac{A_F}{V^{a,b}} \sum_m \frac{-\omega^2 \overline{q}_m L_{nm}^{a,b}}{(-\omega^2+\omega_n^{Aa,b^2})} \tag{11}$$

Substitution of (10) and (11) into (9) gives (before substitution one should replace the summation index, m, in (11) by r to avoid confusion with the m in (9))

$$\sum_m \overline{q}_m Q_{rm} = 0 \qquad r = 1,2,3,\ldots$$

where

$$Q_{rm} \equiv \frac{1}{V^a} \sum_n \frac{L_{nr}^a L_{nm}^a}{M_n^a[-\omega^2+\omega_m^{Aa^2}]} + \frac{1}{V^b} \sum_n \frac{L_{nr}^b L_{nm}^b}{M_n^b[-\omega^2+\omega_m^{Ab^2}]} \tag{12}$$

The natural frequencies are determined by the condition that the determinant of coefficients must vanish

$$| Q_{rm} | = 0 \tag{13}$$

(13) is a non-standard eigenvalue problem because of the form that ω^2 takes in Q_{rm}, see (12). However, it has one overwhelming advantage as compared to the standard (modified for gyroscopic coupling[8]) eigenvalue approach embodied in (7) and (8): The size of the matrix in (13) will be much smaller than that in (7) and (8). This is because the number of <u>two-dimensional</u> opening modes, ψ_m, may be much smaller than the number of <u>three-dimensional</u> cavity modes, F_n^a, F_n^b, to achieve a given level of accuracy. This advantage will persist even when the opening is a structural member of finite stiffness and mass, but the

mathematics are a bit more cumbersome.

In closing this section we quote, without detailed derivations, two generalizations of the above results.

For an external wall of cavity a whose motion, w^{Ea}, is prescribed (sinusoidal motion is assumed for simplicity)

$$w^{Ea} = \sum_m q_m^{Ea} \psi_m \tag{14}$$

The equation of motion is

$$\sum_m \ddot{q}_m Q_{rm} + \ddot{Q}_r^E = 0 \tag{15}$$

where $\ddot{Q}_r^E \equiv \frac{A_{Ea}}{V_a} \sum_n \sum_k \frac{\ddot{q}_k^{Ea} L_{nk}^{Ea} L_{nr}^{a}}{M_m^{Aa}[-\omega^2+\omega_m^{Aa^2}]}$

Forced motion will be discussed in much greater depth in Section VI.

For three cavities, a, b, and c, which are interconnected by openings (all other walls rigid) the counterpart of equation (12) becomes

$$\sum_m \ddot{q}_m^{ab} Q_{rm}^{ab} + \sum_m \ddot{q}_m^{bc} Q_{rm}^{bc(ab)} = 0$$

$$\sum_m \ddot{q}_m^{ab} Q_{rm}^{ab(bc)} + \sum_m \ddot{q}_m^{bc} Q_{rm}^{bc} = 0$$

where

$$Q_{rm}^{ab} \equiv -\frac{A_F^{ab}}{V_a} \sum_n \frac{L_{nr}^{a(b)} L_{nm}^{a(b)}}{M_n^{Aa}(-\omega^2+\omega_n^{Aa^2})} - \frac{A_F^{ab}}{V_b} \sum_n \frac{L_{nr}^{b(a)} L_{nm}^{b(a)}}{M_n^{Ab}(-\omega^2+\omega_n^{Ab^2})}$$

$$Q_{rm}^{bc(ab)} \equiv + \frac{A_F^{bc}}{V_b} \sum_n \frac{L_{nr}^{b(a)} \; L_{nm}^{b(c)}}{M_n^{Ab}(-\omega^2+\omega_n^{Ab^2})}$$

$$Q_{rm}^{ab(bc)} \equiv \frac{A_F^{ab}}{V_b} \sum_n \frac{L_{nr}^{b(c)} \; L_{nm}^{b(a)}}{M_n^{Ab}(-\omega^2+\omega_n^{Ab^2})}$$

$$Q_{rm}^{bc} \equiv - \frac{A_F^{bc}}{V_b} \sum_n \frac{L_{nr}^{b(c)} \; L_{nm}^{b(c)}}{M_n^{Ab}(-\omega^2+\omega_n^{Ab^2})}$$

$$- \frac{A_F^{bc}}{V_c} \sum_n \frac{L_{nr}^{c(b)} \; L_{n\,m}^{c(b)}}{M_m^{Ac}(-\omega^2+\omega_n^{Ac^2})} \tag{16}$$

where A_F^{ab} - is area of common opening to cavities a and b, etc. The generalization to any number of interconnected cavities should now be clear.

The relationship of this analysis to other methods also deserves brief mention. Morse and Ingard[6] have considered two coupled cavities employing a Green's Function approach. The final result is the same as that obtained here, (12). See Appendix B for details. Alternatively, in the context of the variational formulation, as far as computing acoustical natural frequencies of multiply connected cavities with pure openings and otherwise rigid walls is concerned, the q_m may be considered a Lagrange multiplier which enforces the constraint that the pressures in cavities a and b must be equal at their common opening. Hence the present analysis may be thought of as a component mode synthesis

where the components are the individual cavities. The results are entirely analogous to those previously obtained in structural vibrations, except the roles of force and deflection are interchanged[14]. In structural applications, the Lagrange multipliers are forces of constraint enforcing common deflections where two structural components are connected; in acoustical applications, the Lagrange multipliers are deflections of constraint which enforce common forces (acoustical pressures) where two acoustical components (cavities) are connected.

With the combined, equivalent single cavity modes determined by the method described in this section, it is sufficient to consider a single cavity in the subsequent discussion of forced response in Section VI.

VI FORCED RESPONSE OF A CAVITY WITH A FLEXIBLE AND/OR ABSORBING WALL

Basic Model

Here a single cavity is considered; multiply connected cavities can be treated by first determining their combined single cavity natural modes as in Section V.

The total pressure loading on the structural wall is now the sum of the internal acoustic cavity pressure and an external (prescribed) pressure loading. Hence, the structural modal equations are

$$M_m[\ddot{q}_m + 2\zeta_m\omega_m \dot{q}_m + \omega_m^2 q_m] = Q_m \tag{1}$$

where $Q_m \equiv \iint_{A_F} p\psi_m \, dxdy$

$$p = p^c + p^E$$

and

$$p^c = \rho_0 c_0^2 \sum_n \frac{P_n F_n}{M_n^A} \tag{2}$$

p^E, the prescribed external pressure, is the new element in the theoretical model. Q_n may be written

$$Q_m = \rho_0 c_o^2 A_F \sum_n \frac{P_n L_{nm}}{M_n^A} + Q^E_m \tag{3}$$

$$\text{where } Q^E_m \equiv - \iint p^E \psi_m \, dxdy \tag{4}$$

Combining (1) and (3),

$$M_m[\ddot{q}_m + 2\zeta_m\omega_m \dot{q}_m + \omega_m^2 q_m] = \rho_0 c_0^2 A_F \sum_n P_n \frac{L_{nm}}{M_n^A} + Q^E_m \tag{5}$$

The cavity modal equations are

$$\ddot{P}_n + \omega_n^{A^2} P_n + A_A \rho_0 c_0^2 \sum_r \frac{\dot{P}_r C_{nr}}{M_r^A} = - \frac{A_F}{V} \sum_m L_{nm} \ddot{q}_m \tag{6}$$

One can write (5) and (6) in an attractive matrix form by again introducing the velocity potential, ϕ. Bernoulli's equation is

$$p = - \rho_0 \dot{\phi} \tag{7}$$

Using an expansion for ϕ,

$$\phi = \sum_n a_n F_n \tag{8}$$

(5) and (6) may be written

$$\begin{bmatrix} M \end{bmatrix} \begin{Bmatrix} \ddot{q} \\ \ddot{a} \end{Bmatrix} + \begin{bmatrix} G \end{bmatrix} \begin{Bmatrix} \dot{q} \\ \dot{a} \end{Bmatrix} + \begin{bmatrix} C \end{bmatrix} \begin{Bmatrix} \dot{q} \\ \dot{a} \end{Bmatrix} + \begin{bmatrix} K \end{bmatrix} \begin{Bmatrix} q \\ a \end{Bmatrix} = \begin{Bmatrix} Q^E \\ 0 \end{Bmatrix} \tag{9}$$

where

$$\begin{bmatrix} M \end{bmatrix} \equiv \begin{bmatrix} M_m & 0 \\ 0 & VM_n^A \end{bmatrix} , \quad \begin{bmatrix} G \end{bmatrix} \equiv \begin{bmatrix} 0 & \rho_0 A_F L_{nm} \\ -c_0 A_F L_{nm} & 0 \end{bmatrix}$$

$$\begin{bmatrix} C \end{bmatrix} \equiv \begin{bmatrix} 2M_m \zeta_m \omega_m & 0 \\ 0 & A_A \rho_0 c_0^2 C_{nr} \end{bmatrix} , \begin{bmatrix} K \end{bmatrix} \equiv \begin{bmatrix} M_m \omega_m^2 & 0 \\ 0 & VM_n^A \omega_n^{A^2} \end{bmatrix}$$

These equations can be solved numerically by standard methods[8]. In the remainder of this section, simplifying assumptions are considered which allow useful but approximate analytical solutions to be obtained. These should suffice for a rough estimate and also serve as a guide for more accurate and more elaborate numerical

solutions. In all cases sinusoidal excitation is assumed, i.e.

$$p^E = \bar{p}^E \; e^{i \omega_E t}$$

where ω_E is the excitation frequency.

Because our model is linear any other time history can be considered through superposition of sinusoidal excitation. Random excitation may be considered using the sinusoidal excitation results and power spectra methods[15].

Simplified Models

One may anticipate the largest response will occur when the excitation frequency is near a structural or cavity resonant frequency.

(1) Exciting Frequency = Structural Wall Resonant Frequency.

If $\omega^E \approx \omega_s$ where s denotes a structural resonant (natural) mode, then only q_s will be important and all other q_n may be neglegted. Then, from (6)

$$\overline{P}_n = -\frac{A_F}{V} \frac{L_{ns}\,\ddot{q}_s}{-\omega_s^2+\omega_n^{A^2}} \tag{10}$$

and from (10) and (1)

$$M_s[\ddot{q}_s+2\zeta_s\omega_s\dot{q}_s+\omega_s^2 q_s] = -\rho_0 c_0^2 A_F^2 \sum_n \frac{L_{ns}^2\,\ddot{q}_s}{M_n^A(-\omega_s^2+\omega_n^{A^2})} + \overline{Q}_s^E e^{i\omega_E t} \tag{11}$$

From the right hand side of (11) it is seen that if $\omega_n^{A^2} > \omega_s^2$, then the n^{tn} cavity mode gives rise to equivalent mass, while if $\omega_n^{A^2} < \omega_s^2$, then the nth cavity mode contributes an equivalent stiffness.

Note that the $n = 0$ cavity mode always contributes equivalent stiffness.

In many practical examples the structural wall resonant frequencies will be unchanged by the cavity per se, e.g. the sum on the right hand side of (11) can be neglected. The circumstances under which this is not true will be considered in Section VI, part (2). Making this assumption for now, from (11) one computes as

$\omega^E \to \omega_s$

$$q_s = \frac{Q_s^E}{M_s[2\ \zeta_s \omega_s^2]i} \tag{12}$$

From (12), (10) and (2), the cavity pressure may be computed

$$p^c = \frac{\rho_0 c_0^2\ A_F}{2\zeta_s i\ V} \sum_n \frac{F_n}{M_n^A} L_{ns} \frac{\frac{Q_s^E}{A_F}}{M_{s/A_F}\ [-\omega_s^2+\omega_n^{A^2}]} \tag{13*}$$

If ω_s^2 << lowest non-zero acoustical resonance, then only $n = 0$ need be considered in (13). Hence (13) simplifies to

$$p^c = -\frac{\rho_0\ V}{m\ A_F} \frac{c_0^2}{\omega_s^2\left(\frac{V}{A_F}\right)^2} \frac{1}{2\zeta_s i} \frac{\int \frac{\psi_s dA}{A_F} \int \frac{p^E \psi_s dA}{A_F}}{\int \frac{\psi_s^2 dA}{A_F}} \tag{14*}$$

Representative numbers are

$$\frac{\rho_0\ V}{m\ A_F} = .1\ , \quad \frac{c_0}{\omega_s \frac{V}{A_F}} = 1\ , \quad \zeta_s = .1$$

$$\int \frac{\psi_s dA}{A_F} = \frac{2}{\pi}\ , \quad \int \frac{\psi_s^2\ dA}{A_F} = 1/2$$

Thus $p^c \approx 5\, p_E$, i.e. typically the sound pressure in the cavity will be larger than the external sound pressure, if $\omega_s < \omega^A$. For $\omega_s > \omega^A$, one must compute p^c from (13) and typically $p^c < p^E$.

(2) Structural Resonant Frequency Changed by Coupling with Cavity Modes.

In most cases where there is a significant change in a structural resonant frequency due to the cavity, only the n = 0 cavity mode will be important. Hence (11) may be simplified to

$$M_s[\ddot{q}_s + 2\,\zeta_s\,\omega_s\,\dot{q}_s + \omega_s^2\,q_s]$$

$$= -\rho_0 \frac{c_0^2}{V} A_F^2 \; L_{0s}^2\, q_s + \overline{Q}_s^E\, e^{i\omega_E t} \tag{15}$$

The effect of the cavity (within our approximations) is to modify the structural stiffness term, i.e. the total term is now

$$M_s\omega_s^2 + \rho_0^2 \frac{c_0^2}{V} A_F \quad L_{0s}^2$$

Hence (15) may be written in the more compact form

$$M_s[\ddot{q}_s + 2\zeta_s\omega_s\,\dot{q}_s + \omega_s^{c^2} q_s] = Q_s^E\, e^{i\omega_E t} \tag{16}$$

where the coupled structural-cavity natural frequency is

$$\omega_s^{c^2} \equiv \omega_s^2 + \frac{\rho_0 c_0^2\, A_F^2\, L_{0s}^2}{M_s\, V} \tag{17}^*$$

(17) generalizes an earlier result by Dowell and Voss[4] for structural-cavity coupling. Using (17) the results in Section VI, part 1, e.g. (13), can now be generalized to include structural-cavity coupling. By

examining the ratio of the two terms in (17), one can assess when cavity effects on structural resonances are important.

$$\left(\frac{\rho_0 c_0^2 A_F}{m V \omega_s^2}\right) \frac{\left[\frac{\iint \psi_s \, dA}{A_F}\right]^2}{\left[\frac{\iint \psi_r^2 dA}{A_F}\right]^2}$$

Using our previous estimates for the integrals, the ratio becomes

$$\left(\frac{\rho_0 c_0^2 A_F}{m V \omega_s^2}\right) \frac{8}{\pi^2}$$

Clearly the lowest frequency structural mode will be most affected by the cavity. In extreme cases 5 more than one structural mode may be significantly affected.

Another less frequent case where the structural frequency may be changed due to acoustic action is when a structural mode frequency and acoustic mode frequency are close together. Clearly this is an undesireable situation, since large sound levels would be anticipated at this double resonance. This special case is considered in (4) below.

(3) Exciting Frequency = Cavity Resonant Frequency.

When $\omega^E \to \omega_n^A$, then P_n will be the dominant pressure mode. But (in the absence of absorbent wall damping) if P_n is finite, then from (6) one concludes that

$$\sum_m L_{nm} \ddot{q}_m = 0 \tag{18}$$

The structural equation, (5), becomes

$$M_m[\ddot{q}_m + 2\zeta_m \omega_m \dot{q}_m + \omega_m^2 q_m] = \rho_0 c_0^2 A_F \frac{P_n L_{nm}}{M_n^A} + Q_m^E \tag{19}$$

Solving (19) for q_m gives

$$\bar{q}_m = \frac{\rho_0 c_0^2 A_F \dfrac{\bar{P}_n L_{nm}}{M_m^A} + \bar{Q}_m^E}{M_m[-\omega_n^{A^2} + 2\zeta_m \omega_m i\omega_n^A + \omega_m^2]} \tag{20}$$

(20) into (18), gives

$$\left[\sum_n \frac{L_{nm}^2}{M_m[-\omega_n^{A^2} + 2\zeta_m \omega_m i\omega_n^A + \omega_m^2]}\right] \frac{\bar{P}_n \rho_0 c_0^2 A_F}{M_n^A} + \sum_n \frac{\bar{Q}_m^E L_{nm}}{M_m[-\omega_n^{A^2} + 2\zeta_m \omega_m i\omega_n^A + \omega_m^2]} = 0 \tag{21}$$

Solving (21) for $\bar{P}_n$,

$$\bar{P}_n = -\frac{M_n^A}{\rho_0 c_0^2 A_F} \sum_m \frac{\dfrac{\bar{Q}_m^E L_{nm}}{M_m[-\omega_n^{A^2} + 2\zeta_m \omega_m i\omega_n^A + \omega_m^2]}}{\displaystyle\sum_m \frac{L_{nm}^2}{M_m[-\omega_n^{A^2} + 2\zeta_m \omega_m \omega_n^A i + \omega_m^2]}} \tag{22}$$

For the <u>special case</u> where $\omega_n^A \equiv \omega_m$ for some m, then the sums can be well approximated by a single term and the above relationship simplifies. Even when $\omega_n^A \neq \omega_m$ for any m, there may be a predominant structural mode in which case the sum could be approximated by a single term. First, however, we digress to consider <u>another important limiting case</u>.

If F_n and p^E are constants over A_F, then a very interesting result obtains, namely

$$Q_m^E = - p^E \int \psi_m dA \quad , \quad L_{nm} = F_n \int_{A_F} \psi_m dA \quad ,$$

the ratio of sums simplifies and using (2) and (22),

$$\left.\frac{p^c}{\rho_0 c_0^2}\right|_{\text{on } A_F} = \sum_n \left.\frac{P_n F_n}{M_n^A}\right|_{\text{on } A_F} = \frac{p^E}{\rho_0 c_0^2} \tag{23}$$

Clearly, if $p^c|_{\text{on } A_F} = p_E$ then $w \equiv 0$!

To see this in detail recall that

$$\frac{p^c}{\rho_0 c_0^2} = \sum_n \frac{P_n F_n}{M_n^A} \tag{2}$$

which can be simplified to

$$\frac{p^c}{\rho_0 c_0^2} = \frac{P_n F_n}{M_n^A} \qquad \text{(for } n^{th} \text{ cavity mode dominant)} \tag{2}$$

Using (4) and (22) in (2) one concludes

$$p^c|_{\text{on } A_F} = + pE \qquad \text{and} \qquad w \equiv 0$$

q.e.d.

Note that if

$$p^E = C\,F_n\Big|_{\text{on } A_F}$$

then the same result holds, namely

$$p^c\Big|_{\text{on } A_F} = p^E \qquad \text{and } w \equiv 0$$

If F_n = constant, but $p^E \neq$ constant,, then a similar calculation gives

$$\frac{p^c}{\rho_0 c_0^2}\Bigg|_{\text{on } A_F} = + \frac{1}{\rho_0 c_0^2} \quad \frac{\sum_n \dfrac{\int p^E \psi_m dA \int \psi_m dA}{M_m\,[\,.\;.\;.\,]}}{\sum_n \dfrac{[\int \psi_m dA]^2}{M_m\,[\,.\;.\;.\,]}} \qquad \text{and } w \neq 0 \tag{23}$$

Note that p^c is constant over A_F. Only if there is a single dominant structural mode will this simplify further. Now return to (22).

Single Dominant Structural Mode:

For a single dominant resonant structural mode, m, (22) becomes

$$\overline{P}_n = -\frac{M_n^A\,\overline{Q}_m^E}{\rho_0 c_0^2\,A_F\,L_{nm}} \tag{24}$$

and $$p^c = F_n \frac{\int p^E\,\psi_m\,dA}{\int F_n\,\psi_m\,dA} \tag{25*}$$

<u>If</u> $p^E = C\,F_n\big|_{\text{on } A_F}$, then $p^c = p^E$ on A_F and $w \equiv 0$ as before.

Note that, within reason, ψ_m may be selected as an appropriate linear combination of natural modes. Hence a dominant structural mode assumption

is quite useful.

The central conclusion to be drawn from the above is that, in simple terms, we may think of the cavity as acting as a vibration absorber for the structural wall when the external exciting frequency is equal to the cavity resonance frequency. Hence, at most, the internal cavity pressure will be equal to the external pressure and indeed, if $\omega_m >> \omega_n^A$ for all m, and/or p^E varies significantly over the flexible wall, then $p^c << p^E$.

(3a) Effect of Cavity Wall Absorbtion (Damping).

In our model the absorbtion characteristics are modeled by an impedance, z_A. For representative acoustical materials[16]

$$\frac{z_A}{\rho_0 c_0} = 1\text{-}10$$

Again we shall assume a single cavity mode dominates. Then an equivalent damping ratio of the usual type may be defined

$$2\,\zeta_n^c \equiv \frac{\rho_0 c_0^2}{V}\,\frac{A_A}{\omega_n^A}\,\frac{C_{nn}}{M_n^A}$$

or $$2\,\zeta_n^c = \frac{\rho_0 c_0}{z_A}\,\frac{c_0}{V}\,\frac{A_A}{\omega_n^A}\,\frac{\iint_{A_A} F_n F_n\, dA}{\iiint_V F_n^2 dV}$$

Typically ζ_n^c would be .03 - .3.

Using an equivalent ζ_m^c, (6) becomes

$$\ddot{P}_n + 2\,\zeta_n^c\,\omega_n^A\,\dot{P}_n + \omega_n^{A^2}\,P_n$$

$$= -\frac{A_F}{V}\sum_m L_{nm}\,\ddot{q}_m \qquad (6a)$$

As $\omega^E \to \omega_n^A$, (6a) becomes

$$2\,\zeta_n^c\, i\, \overline{P}_n = \frac{A_F}{V} \sum_m L_{nm}\, \overline{q}_m \tag{26}$$

Using (20) in (26),

$$\frac{V}{A_F}\, 2\,\zeta_n^c\, i\, \overline{P}_n = \rho_0 c_0^2\, A_F \left[\frac{\sum_m L_{nm}^2}{M_m[-\omega_n^{A^2} + 2\zeta_m \omega_m \omega_n^A i + \omega_m^2]} \right] \cdot \frac{\overline{P}_n}{M_n^A}$$

$$+ \sum_m \frac{\overline{Q}_m^E\, L_{nm}}{M_m[-\omega_n^{A^2} + 2\zeta_m \omega_m i \omega_n^A + \omega_m^2]} \tag{27}$$

For $\omega_n^A \cong \omega_m$, retain only one term in sums and thus

$$-4\omega_n^{A^2} \zeta_m \zeta_n^c \frac{V}{A_F}\, \overline{P}_n\, M_m = \rho_0 c_0^2\, A_F\, L_{nm}^2 \frac{\overline{P}_n}{M_n^A} + \overline{Q}_m^E\, L_{nm} \tag{28}$$

Solving,

$$\overline{P}_n = -\frac{\overline{Q}_m^E\, L_{nm}}{\rho_0 c_0^2\, A_F \dfrac{L_{nm}^2}{M_n^A}} \cdot \frac{1}{\left[1 + \dfrac{\omega_n^{A^2}\, 4\zeta_m \zeta_n^c V M_m M_n^A}{\rho_0 c_0^2\, A_F^2\, L_{nm}^2} \right]} \tag{29}$$

Hence effect of cavity damping is to decrease internal pressure field.

However, the numerical effect is typically small.

(4) Exciting Frequency = Structural Wall and Cavity Resonant Frequencies in Close Proximity.

For simplicity we ignore any absorbing wall and consider a single dominant structural wall mode and also a single dominant cavity mode whose natural frequencies are very near each other. From (9) the equations of motion are

$$- M_m[\ddot{q}_m + 2\zeta_m\omega_m \dot{q}_m + \omega_m^2 q_m] + Q_m^E - A_F\rho_0\dot{a}_n L_{nm} = 0 \tag{30}$$

$$VM_n^A [\ddot{a}_n + \omega_n^{A2} a_n] - c_0^2 A_F \dot{q}_m L_{nm} = 0 \tag{31}$$

For a single cavity mode

$$p^c = - \rho_0 \dot{a}_n F_n \tag{32}$$

(30), (31) and (32) may be solved to obtain

$$\frac{\overline{p}^c}{\dfrac{\overline{Q}_E}{L_{nm}A_F}} = \frac{\lambda \Omega_m^{E2} F_n}{\left\{[-\Omega_m^{E2} + 2\zeta_m\Omega_m^E i + 1][-\Omega_m^{E2} + \Omega_m^{A2}] - \lambda\Omega_m^{E2}\right\}} \tag{33}$$

where $\Omega_m^E \equiv \omega^E/\omega_m$

$\Omega_m^A \equiv \omega_n^A/\omega_m$

$\lambda \equiv \dfrac{\rho_0 c_0^2 A_F^2 L_{nm}^2}{VM_n^A M_m \omega_m^2}$

Note that

$$\lambda \sim \frac{\rho_0 V}{\dot{m}\, A_F} \left[\frac{A_F}{V} \frac{c_0}{\omega_m}\right]^2$$

From (33) the coupled structural-acoustic resonant frequencies may be determined and the associated cavity pressure. For the special case of

$$\Omega^A_m = 1$$

and $\lambda << 1$ (typically $\lambda \leq 1$)

particularly simple results may be obtained. The resonant frequencies are then

$$\Omega^E_m \cong 1 \pm \lambda^{1/2} \tag{34}$$

and the cavity pressure at resonance

$$\left| \frac{\dot{p}^c}{\frac{\overline{Q}_E}{L_{nm} A_F}} \right| \cong \frac{\lambda^{1/2}}{2\, \zeta_m} F_n \tag{35*}$$

The left hand side of (35) is approximately p^c/p^E. Hence for typical ζ_m and λ not too small, $p^c/p^E > 1$ when a cavity and structural wall mode coincide in natural frequencies.

(5) Convection Effects on External Sound Sources and Internal Sources.

The results discussed to this point are for a stationary external sound source. Here a few brief (cautionary) comments are offered with respect to other sound sources.

If substantial convection of an external sound source is present,

hydrodynamic coincidence effects may occur and also radiation damping in the external flow may be important[17].

For sound sources inside the cavity itself, the wall absorbtion will play a much more important role than for the external sound sources studied here[16].

(6) Summary of Key Relations from Simplified Models to Determine Cavity Pressure.

Exciting frequency = structural wall resonant frequency.

For $\omega^E \to \omega_s$, (13)* or (14)* modified by (17)* as necessary.

Exciting frequency = cavity resonant frequency.

For $\omega^E \to \omega_n^A$, (single dominant structural mode) (25)*

Exciting frequency = structural wall and cavity resonant frequencies in close proximity.

For $\omega^E \to \omega_s \equiv \omega_n^A$, (35)*.

When the external excitation frequency is well separated from all structural or cavity resonant frequencies, there may not be a single dominant structural and/or cavity mode. However, some simplification may still be possible by neglecting the interaction between structural wall and cavity, i.e. one may first determine the structural wall motion and then use that result to determine the internal cavity acoustic pressure. In this approximation the effect of the cavity sound pressure on the structural wall motion is omitted.

It is also worth emphasizing that for off-resonant exciting frequencies, although the numerics may be more elaborate due to the necessity of accounting for multiple modes, the basic theoretical model may be more accurate because the uncertainty with respect to structural and/or acoustic damping values will be less important.

VII NUMERICAL RESULTS AND COMPARISONS WITH EXPERIMENTS

For a single cavity with a flexible wall and an external sound source, the theoretical model has been verified experimentally by several authors[4,5,18,19,20,21].

Here we assess the capability of the model to describe accurately the acoustic natural modes in multiply connected cavities. Once the combined natural modes of the multiply connected cavities are determined and verified experimentally, they may be treated as one single cavity. Hence the earlier work for a single cavity[4,5,18,19,20,21] then may be taken as experimental verification for the forced excitation of multiply connected cavities as well.

Acoustic Natural Modes in Multiply Connected Cavities.

The experimental studies were conducted by Smith[22] who has considered several geometrical arrangements for two acoustic cavities with rigid walls and a partial opening between them, see Fig.1. In Fig.2 the lowest found longitudinal resonant frequencies from theory (Section V) and experiment are shown vs partition size, y_c, normalized by cavity height, d. As may be seen the agreement is good with the exception of the 10* mode for $\Omega \approx .4$ where a mechanical resonance of the loudspeaker used to excite the acoustic modes contaminates the data. In practical terms this is unavoidable as both theory and experiment show that $\Omega_{10} = .5 \rightarrow 0$ as the partition is closed, $y_c/d = 0 \rightarrow .5$. In these experiments, $c_0 = 1117$ ft/sec, a = d = 10" and the width dimension was 4" to provide two-dimensional conditions in the frequency range of interest. The thickness of the partition (assumed

*10 means there is 1 longitudinal nodeline and 0 lateral notelines, etc.

zero in the theoretical calculations) is .5" as is the thickness of all external walls. The cavity is constructed from plexiglass.

In Figure 3 for a constant aperture (opening) size, $y_{a/d} = .5$, the effect of aperture location is studied. Both theory and experiment show a small effect.

A second configuration studied by Smith consists of two acoustic cavities, one twice the dimensions of the other, with rigid walls and a partial opening between them. In Figure 4 the lowest four longitudinal resonant frequencies from theory and experiment are shown vs. normalized partition size, $y_{c/d}$. Again the agreement is good. In Figure 5, the longitudinal pressure distributions (along with their resonant frequencies) are shown for the first seven (symmetric with respect to height) acoustical modes with a full opening between cavities. The agreement between theory and experiment is very good.

Altogether one concludes the theoretical results are a faithful description of the physical model. For more detail the reader should consult Reference 22.

Forced Response of a Cavity with a Flexible Wall

Experimental Arrangement:

For this discussion, Gorman's work[18,19] is used; however, also see Reference 4,5,20 and especially 21. The experimental arrangement is shown in Figure 6. The flexible wall panel was a 10" x 20" x 0.05" aluminum alloy plate that was bonded onto a rectangular frame consisting

of aluminum channel members welded together at their ends. By bonding the plate to the cavity in this way, a clamped edge boundary condition was approximated. A sealed cavity, also 10" x 20", was constructed beneath the panel in such a way that the cavity depth could be varied in 2 inch increments from 12" to 2" deep. The cavity itself was made of 0.5" thick plexiglass and was supported by four plexiglass "feet".

The panel was excited acoustically by a Wolverine LS15, 20 watt loudspeaker driven by a B & K Beat Frequency Oscillator, type 1022. The external sound field was set at 100 dB at the mid-point on the plate surface for all measurements. By using a single speaker, an external field distribution that was variable in space was obtained. See Figure 7.

Initially, there were two basic measurements that were felt to be important: the measurement of panel amplitude and the measurement of cavity pressures due to a sinusoidal driving force. As work progressed, however, the need arose for two more measurements: the measurement of panel and cavity damping ratios. The reasons for these latter measurements will become apparent later.

Panel Amplitude Measurement:

The panel motion was measured by the use of a Bently Nevada motion pickup, Model 302, that was mounted on an aluminum frame located above the panel. The frame allowed movement of the pickup to any point on the surface of the panel, and also allowed variation of the distance between the pickup and the panel. As the panel oscil-

lated, the voltage generated by the motion pickup was fed through an amplifier and recorded on a amplitude vs. frequency plot. Such a plot is shown in Figure 8, for a cavity depth of 12".

For the measurement depicted in Figure 8, the motion pickup was positioned at the center of the panel. By positioning the pickup in this way, one may obtain deflection measurements for the symmetric panel modes, i.e., the modes which have a peak at the panel center, but not for the antisymmetric modes, i.e., those modes with a node at the panel center. The dominant features of the plot are the three resonant peaks, corresponding to the first, third and fifth panel modes, occuring at 113 cps, 210 cps and 410 cps. Modes above the fifth mode have an amplitude that is negligible compared to the first three symmetric modes. Above 500 cps, the panel is essentially motionless. The dominant panel response is at the panel fundamental mode, as is expected.

Cavity Pressure Measurement:

The sound pressure level within the cavity, when the panel has been excited by the loudspeaker, was measured using a B & K 1/4" microphone, Type 4136 with a Type 2615 cathode follower with Type UA 0035 connector. This microphone was installed in holes that were drilled in the side of the cavity. As with the panel motion pickup, the voltage from the microphone due to excitation of the cavity was recorded on a amplitude vs. frequency plot. Such a plot is shown in Figure 9, for a cavity depth of 12".

For the measurement depicted in Figure 9, the microphone was positioned in the hole located at the 3" cavity depth level. Since all theoretical calculations involve the cavity pressure at a point just beneath the panel, the 3" depth level was chosen to place the

microphone as close to the undersurface of the panel as possible.

In Figure 9, the cavity pressure is plotted against frequency, where this pressure is the difference between the dB level inside the cavity and the dB level outside the cavity on the upper surface of the panel. Again, the dominant features are the three primary resonant peaks occuring at 113 cps, 210 cps and 518 cps. The first two resonances correspond to the first and third panel modes, and thus indicate that the panel is driving the cavity at these frequencies. The resonance at 518 cps is the fundamental cavity mode. Note that this mode occurs above the frequency at which the panel becomes motionless (500 cps), and thus, in effect, the cavity is acting as a rigid cavity with no flexible walls. Theoretically, since the panel is motionless, the pressure level difference between the external and internal measurements should be zero. This is practically the case in Figure 9, the slight variation from zero due to the very slight motion of the panel at this frequency. Note also, that, as with the panel amplitude, the greatest cavity response occurs at the panel fundamental frequency, with the second greatest response occurring at the cavity fundamental frequency.

Damping Ratio Measurement:

The damping ratios of the panel and cavity can be measured experimentally in two different ways: the first, by using the "peak method", and the second, by using the "decay method". The decay method was the method used to determine experimentally damping ratios.

The actual measurement of damping ratios was as follows: using an oscillograph, a plot of amplitude vs. time was obtained. As the oscillograph was recording, the voltage to the loudspeaker was cut off, thus eliminating the external sound field, and the classic exponential decay plot was obtained.

Figure 10, plots the damping ratio of the panel with a 12" deep cavity as a function of frequency. The experimental points were measured at the first, third and fifth panel modes for this panel - cavity configuration. The curve obtained is consistent with a theoretical model, which says that for damping that is proportional to panel velocity, the damping ratio varies as the inverse of the frequency. The slight variation from theory at the higher panel frequencies is probably due to coupling between the panel and cavity modes.

Figure 11, plots the damping ratio of the cavity (12" depth) as a function of frequency. The experimental points were measured at the first, second and third cavity depth modes. The curve obtained suggests that the cavity damping ratio at a constant cavity depth varies as the inverse of the frequency squared. This result is inconsistent with Sheshadri[23], concerning the damping of Helmholtz resonators, and also does not agree with the variation of panel damping with frequency at a constant cavity depth. As yet, no explanation can be given for this damping result, other than to conclude that such a result seems to indicate a more complex damping mechanicsm than that of the panel. For the panel, the damping was assumed to be proportional to the

velocity of the panel. For the cavity, such a simple relationship cannot be assumed.

Results:

Panel Frequency Response

Since the panel-cavity system being discussed is an integrated system, one must investigate the coupling effects between the panel and cavity. It is well known that the cavity effect on the panel will become more pronounced as the cavity depth decreases.[4,5,20,21] In Figure 12, the panel deflection, normalized about the mid-point of the panel, has been plotted against the panel length, normalized with the total panel length, for the fundamental mode of the panel backed up by a 12" and a 2" deep cavity. Figure 13, plots a similar response, only normalized about the one-third point of the panel, for the third panel mode. These graphs depict the effect of intermodal coupling at shallow cavity depths. The panel response at the 12" depth for both the first and third panel modes is very close to the "in-vacuo" curve given by Dowell and Voss,[21] inter alia, indicating that a 12" deep cavity approximates an infinite cavity fairly effectively for the panel size investigated here.

For a cavity depth of 2", the mode shapes vary considerably. In the case of the panel fundamental mode, the response is more concentrated about the center of the panel than for the 12" depth case. The response can be seen to be approaching the shape of the third mode, indicated intermodal coupling at this shallow cavity depth. Indeed, if the cavity was made more shallow, the panel fundamental mode would take on the modal pattern of the third mode by having two

nodal points[4,21]. For the third panel mode at the 2" cavity depth, the change in modal shape is less dramatic. However, there is some effect, especially around the mid-point of the panel, and this measured effect corresponds to the results of Dowell and Voss. Again, if the cavity were made more shallow, the effect would be more dramatic with the probable elimination of all nodal points, indicating intermodal coupling between the first and third panel modes.

Aside from affecting the mode shapes of the panel, the cavity also affects the natural frequencies of the panel due to the stiffness and virtual mass effects discussed previously. In Figure 14, the panel fundamental frequency is plotted against cavity depth. Note that, as the cavity depth decreases, the panel fundamental frequency is an excellent example of the stiffness effect, for, as the cavity depth is decreased, the cavity becomes stiffer, thus raising the panel natural frequency. Figure 15, plots the panel frequencies vs. cavity depth for the third and fifth panel modes. Note that there is apparent a slight stiffness effect on the third mode, and the lack of any stiffness effect on the fifth mode. In fact, the fifth panel mode displays features of the virtual mass effect, for as the cavity depth decreases, the natural frequencies decrease also. This fact also indicates that the virtual mass effect is present in symmetric panel modes, and not just in the antisymmetric modes. The frequency response for the third and fifth panel modes is consistent with theory, which states that the stiffness effect becomes less for the higher symmetric modes and that the virtual mass effect is present in all modes.[4,5,21].

In Figure 16, a comparison between theory and experiment is made. The ratio of panel frequency (modified by coupling with the cavity) to "in-vacuo" panel frequency is plotted against panel length to cavity depth ratio, a/d. The "in-vacuo" panel frequencies were computed from Warburton's theory,[24] and the panel frequencies' variation with cavity depth were computed from Dowell and Voss' theory[21] which is an earlier version of the present analysis. There is excellent agreement between theory and experiment at the large cavity depths, with some variation from theory occurring at shallow cavity depths. One or two panel modes plus the cavity Helmholtz mode were used in the calculation. This agreement between theory and experiment seems to indicate that below an a/d of 10, for a panel with similar size, thickness and material properties as the one investigated here, a one-term panel mode approximation to the panel natural frequencies may be used with good accuracy. For a/d > 10, higher term approximations must be employed. More generally, for $\lambda_c a/d > 10{,}000$ higher term approximations must be used to compute panel natural frequencies for a panel length to width ratio, $a/_b$, of two.[5,20]

Cavity Frequency Response

The cavity also responds in certain characteristic modes. Theoretically, at low frequencies below the cavity fundamental, the cavity pressure should be constant over the cavity depth since the cavity is responding in its Helmholtz mode. Figure 17, plots the cavity pressure, normalized with the external pressure, along the cavity depth at the panel fundamental frequency. Apparent is the fact that the cavity pressure distribution is not exactly constant, but is approximately so.

Figure 18, plots a similar normalized pressure distribution at the cavity fundamental depth frequency. Theory predicts that the cavity should respond in a cosine mode, with the internal and external pressures equal at the top and bottom of the cavity, and with the response undergoing a phase shift with cavity depth. Note that the experimental pressure distribution in the cavity at the cavity depth fundamental follows the theoretical cosine courve fairly well except at the deepest part of the cavity.

Panel Displacement and Damping Effect

There are three types of damping that will be referred in this discussion: constant damping, frequency damping, and experimental damping. Constant damping is the value measured for d = 12" and assumes that there is no variation of panel modal damping ratio with cavity depth. Frequency damping allows for variation of damping ratio with frequency and employs the data measured at a 12" cavity depth for various panel resonances. Thus, the only effect changing this type of damping is the variation of panel modal frequency with cavity depth. Experimental damping is the damping ratio measured for the exact conditions under investigation.

Figure 19, plots the panel damping ratio due to the effect of increasing frequency alone, and from experiment. Note that the frequency effect forces the panel damping ratios lower, whereas, the experimental damping ratios are higher, as the cavity depth is reduced. The reasons for this behavior not readily apparent; however, it is felt that, if there were some leakage from the cavity thus creating more losses in the system, the effect would be to make

the panel respond less ideally, i.e., to increase the damping ratio. Experiments show that the cavity pressure increases with a decrease in cavity depth. Thus, if there were a leak present, the effect would be greatest at the shallow cavity depths. This reasoning is consistent with the experimental results depicted in Figure 19.

With the panel damping ratios determined, the theory may be used to compute a one-term solution for the panel amplitude, for three cases: constant damping, frequency damping and experimental damping. These results have been plotted in Figure 20, along with the measured panel amplitudes. The constant damping and frequency damping cases predict the correct panel amplitudes only at large cavity depths; however, the experimental damping ratios predict the panel amplitudes well throughout the range of cavity depths tested. From this, one may conclude, that, given the proper damping ratios, a one-term approximation for the panel amplitudes is accurate within the range of cavity depths tested.

A similar result was seen[18] for panel amplitudes for the third and fifth panel modes. Again, the experimental damping ratio predicted the panel amplitudes more accurately than the frequency damping effect.

Cavity Pressure and Damping Effects

As with the panel amplitude, the theory may be used to compute cavity pressures. Figure 21, plots the variation of cavity pressure with cavity depth for constant damping effect, frequency damping, and experimental damping. The exciting external frequency is equal to the panel resonant frequency. Recall that the damping ratios used in these calculations are the effective panel damping ratios and not

those of the cavity; the latter were neglected. Even though cavity damping has not been considered, there is excellent agreement between experiment and the experimental damping case. This indicates that, for the fundamental panel mode, and the range of cavity depths tested, the use of one-term panel theory, the Helmholtz cavity mode and only panel damping ratios will predict cavity pressures accurately.

Similar results have been obtained for random external pressure excitation[19]. Pretlove[5] has made measurements of panel natural frequency variation with cavity depth; Guy and Bhattacharya[21] have measured cavity pressures and panel natural frequencies. Generally good agreement with theory has also been shown in Ref. 5, 19 and 21.

VIII CONCLUDING REMARKS

A comprehensive theoretical model is developed for interior sound fields which are created by flexible wall motion resulting from exterior sound fields. Including in the model are the mass, stiffness and damping characteristics of the flexible wall as well as the mass, stiffness, and damping (due to absorbing interior walk) of the acoustic cavity. Full coupling between the wall and cavity is permitted although detailed analysis, numerical results and experiment suggest that it is the exceptional (though perhaps occasionally important) case when the structural wall dynamics characteristics are significantly modified by the cavity.

Based upon the general theory, an efficient computational method is proposed and used to determine acoustic natural frequencies of multiply connected cavities.

Simplified formulae are developed for interior sound levels in terms of in-vacuuo structural wall and (rigid wall) acoustic cavity natural modes.

Comparisons of theory with experiment show generally good agreement. The principal uncertainty remains the structural and/or cavity damping mechanisms. For external sound excitation, cavity damping is demonstrated to be generally unimportant; however, it may be of substantial importance for interior sound sources. No systematic experimental data are available for cavity damping to assess the validity of the present theoretical

model in this respect.

The results of the present work, as well as those of Wolf, Nefske and Howell[25] using finite element techniques and Howlett and Morales[26] (based upon earlier work by Cockburn and Jolly[27]) using modal analysis for a particular wall and cavity geometry, suggest that effective analytical models are available subject to the uncertainties concerning damping previously discussed. For a further entree to the literature one may consult Reference 25 and additional references cited therein as well as the recent work by Petyt, Lea and Koopman.[28]

REFERENCES

1. Junger, M. and Feit, D., "Sound, Structures and Their Interaction", M.I.T. Press, 1972.
2. Dowell, E. H., "Aeroelasticity of Plates and Shells", Noordhoff International Publishing, Leyden, 1974.
3. Kinsler, L. E. and Frey, A. R., "Fundamentals of Acoustics", John Wiley, 1950.
4. Dowell, E. H. and Voss, H. M., "The Effect of a Cavity on Panel Vibrations", AIAA Journal, 1, pp.476-477, 1963.
5. Pretlove, A. J., "Free Vibrations of a Rectangular Panel Backed by a Closed Rectangular Cavity", J. Sound Vib. 2, pp.197-209, 1965.
6. Morse, P.M. and Ingard, K. Y., Theoretical Acoustics, Mc Graw-Hill, New York, 1968.
7. Dowell, E. H., "Transmission of Noise from a Turbulent Boundary Layer Through a Flexible Plate into a Closed Cavity", J. Acoustical Soc. Am., 46, pp.238-252, 1968.
8. Meirovitch, L., "A New Method of Solution of the Eigenvalue Problem for Gyroscopic Systems", AIAA Journal, 12, pp.1337-1342, 1974.
9. Gladwell, G. M. L. and Zimmermann, "On Energy and Complementary Energy Formulations of Acoustic and Structural Vibration Problems", J. Sound Vib., 3, pp. 233-241, 1966.
10. Gladwell, G. M. L., "A Variational Formulation of Damped Acousto-Structural Vibration Problems", J. Sound Vib., 4, pp.172-186, 1966.

11. Gladwell, G. M. L. and Mason, V., "Variational Finite Element Calculation of Acoustic Response of a Rectangular Panel", J. Sound Vib., 14, pp. 115-135, 1971.

12. Craggs, A., "The Transient Response of a Coupled Plate-Acoustic System Using Plate and Acoustic Finite Elements", J. Sound Vib., 15, pp. 509-528, 1971.

13. Craggs, A., "An Acoustic Finite Element Approach for Studying Boundary Flexibility and Sound Transmission Between Irregular Enclosures", J. Sound Vib., 30, pp. 343-357, 1973.

14. Dowell, E. H., "Free Vibrations of an Arbitrary Structure in Terms of Component Modes", J. of Applied Mechanics, 39, pp.727-732, 1972.

15. Lin, Y. K., "Probabilistic Theory of Structural Dynamics", McGraw-Hill, 1967.

16. Beranek, L. L., "Noise Reduction", McGraw-Hill, 1960.

17. Maestrello, L., "Measurement and Analysis of the Response Fields of Turbulent Boundary Layer Excited Panels", J. Sound Vib., 2, pp. 270-292, 1965.

18. Gorman, III, G. F., "An Experimental Investigation of Sound Transmission Through a Flexible Panel into a Closed Cavity", Princeton University AMS Report No. 925, July 1970.

19. Gorman, III, G. F., "Random Excitation of a Panel-Cavity System", Princeton University AMS Report No. 1009, July 1971.

20. Dowell, E. H. and Voss, H. M., "Experimental and Theoretical Panel Flutter Studies in the Mach Number Range of 1.0 to 5.0", AIAA Journal, 3, pp. 2292-2304, 1965.

21. Guy, R. W. and Bhattacharya, M. C., "The Transmission of Sound Through a Cavity-Backed Finite Plate", J. Sound Vib.27, pp.207-223, 1973.

22. Smith, D.A., "An Experimental Study of Acoustic Natural Modes of Interconnected Cavities", Princeton University AMS Report No. 1284, August 1976.

23. Sheshadri, T. V., "Transient Response of Mechano-Acoustical Networks", Ph.D. Thesis, Oklahoma State University, 1968.

24. Warburton, G. B., "The Vibration of Rectangular Plates", Proc. Inst. Mech. Engrs. (London), 168, pp. 391-384, 1954.

25. Wolf, Jr., J. A., Nefske, D. J., and Howell, L. J.,"Structural-Acoustic Finite Element Analysis of the Automobile Passenger Compartment", SAE Paper 760184, Presented at the Automotive Engineering Congress and Exposition, Detroit, Michigan, February 1976.

26. Howlett, J. T. and Morales, D.A., "Prediction of Light Aircraft Interior Noise", NASA TM X-72838, April 1976.

27. Cockburn, J. A., and Jolly, A. C., "Structural Acoustic Response, Noise Transmission Losses and Interior Noise Levels of an Aircraft Fuselage Excited by Random Pressure Fields", Air Force Flight Dynamics Laboratory Technical Report, AFFDL-TR-68-2, August 1968.

28. Petyt, M., Lea, J. and Koopman, G. H., "A Finite Element Method for Determining the Acoustic Modes of Irregular Shaped Cavities", J. Sound Vib. 45, pp.495-502, 1976.

APPENDIX A

ACOUSTIC NORMAL MODES OF A CAVITY WITH RIGID WALLS.

Here we consider a representative, but simple, calculation of acoustical normal modes.

Normal Modes of a Rectangular Acoustic Cavity

We shall seek non-trivial (i.e. non-zero) solutions for a cavity with rigid walls. As usual the equation of motion is

$$\nabla^2 p - 1/c_o^2 \frac{\partial^2 p}{\partial t^2} = 0 \qquad (1)$$

with the boundary condition

$$\frac{\partial p}{\partial n} = 0 \text{ on all (rigid) walls} \qquad (2)$$

where n is coordinate normal to any wall. For a rectangular cavity with dimensions and coordinates shown below,

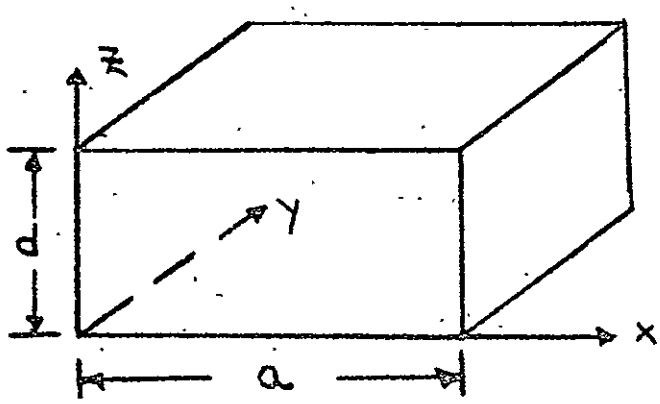

the boundary conditions are

$$\frac{\partial p}{\partial x} = 0 \quad \text{on } x = 0,\ a$$

$$\frac{\partial p}{\partial y} = 0 \quad \text{on } y = 0,\ b \qquad (2)$$

$$\frac{\partial p}{\partial z} = 0 \quad \text{on } z = 0,\ d$$

We assume simple harmonic motion

$$p(x,y,z,t) = F(x,y,z)\ e^{i\omega t} \tag{3}$$

and seek the frequencies, $\omega = \omega_m$, for which non-trivial solutions are possible. These are called the normal mode (or natural) frequencies. Mathematically speaking they are the eigenvalues of the problem. The corresponding solutions for F, $F = F_m(x,y,z)$ are the normal or natural modes or eigenfunctions. Assuming a separable solution for F,

$$F(x,y,z) = X(x)\ Y(y)\ Z(z) \tag{4}$$

we may substitute (3) and (4) into (1) to obtain (subscripts denote differentiation with respect to that variable)

$$\frac{X_{xx}}{X} + \frac{Y_{yy}}{Y} + \frac{Z_{zz}}{Z} + \left(\frac{\omega}{c_0}\right)^2 = 0 \tag{5}$$

Introducing separation constants, k_x, k_y, (5) becomes

$$\frac{X_{xx}}{X} = -k_x^2$$

$$\frac{Y_{yy}}{Y} = -k_y^2 \tag{6}$$

$$\frac{Z_{zz}}{Z} = k_x^2 + k_y^2 - \left(\frac{\omega}{c_0}\right)^2 \equiv -k_z^2$$ (This defines k_z in terms of ω and vice versa):

Solving (6)

$$X = A \cos k_x x + B \sin k_x x$$

$$Y = C \cos k_y y + D \sin k_y y$$

$$Z = E \cos k_z z + F \sin k_z z \tag{7}$$

To determine the constants, A, B, etc., k_x, etc., we satisfy the boundary conditions (2). In terms of X, Y, Z, these are

$$X_x = 0 \quad \text{on } x = 0, a$$

$$Y_y = 0 \quad \text{on } y = 0, b$$

$$Z_z = 0 \quad \text{on } z = 0, d \tag{8}$$

Using (7) and the first of these we have

$$k_x [-A \sin k_x x + B \cos k_x x] = 0 \quad x = 0, a$$

$$\text{or} \quad k_x B = 0 \tag{9}$$

and $k_x [-A \sin k_x a + B \cos k_x a] = 0$

Thus $B = 0$ and either

$$A = 0 \ \underline{\text{or}} \tag{10}$$

$\sin k_x a = 0 \rightarrow k_x a = 0, \pi, 2\pi, 3\pi, \ldots$

The latter is the alternative which corresponds to non-trivial solutions. The corresponding X is

$$X = A \cos k_x x = A \cos \frac{m_x \pi x}{a}, \text{ where } m_x = 0,1,2,3,\ldots \tag{11}$$

Similarly for Y and Z

$$k_y b = m_y \pi \ , \ m_y = 0,1,2,\ldots$$

$$Y = C \cos \frac{m_y \pi y}{b} \tag{12}$$

$$k_z d = m_z \pi \ , \ m_z = 0,1,2,\ldots$$

$$Z = E \cos \frac{m_z \pi z}{d}$$

Hence from (4) and (6), using (10), (11), (12),

$$F_m(x,y,z) \sim \cos \frac{m_x \pi x}{a} \cos \frac{m_y \pi y}{b} \cos \frac{m_z \pi z}{d} \tag{13}$$

and $\frac{\omega_m^2}{c_0^2} = \pi^2 \left[\left(\frac{m_x}{a}\right)^2 + \left(\frac{m_y}{b}\right)^2 + \left(\frac{m_z}{d}\right)^2\right]$

Note F_m is only determined to within an arbitrary constant. Also we use for shorthand a single modal subscript , m , on F_m and ω_m. Of course, each m corresponds to a single triplet combination of integers, m_x, m_y, m_z.

One of the most interesting and useful properties of the F_m is their "orthogonality", i.e.

$$\iiint F_m F_n \, dxdydz = 0 \text{ for } m \neq n \tag{14}$$

This can be proved most directly using Green's Theorem for F_m and F_n.

$$\iiint [F_n \nabla^2 F_m - F_m \nabla^2 F_n] dxdydz$$
$$= \iint [F_n \frac{\partial F_m}{\partial n} - F_m \frac{\partial F_n}{\partial n}] \, dA \tag{15}$$

Now $\frac{\partial F_m}{\partial n} = \frac{\partial F_n}{\partial n} = 0$ from (2)

and $\nabla^2 F_m = -\left(\frac{\omega_m}{c_0}\right)^2 F_m$ from (1)

$\nabla^2 F_n = -\left(\frac{\omega_n}{c_0}\right)^2 F_n$

Hence (15) becomes

$$(\omega_n^2 - \omega_m^2) \iiint F_n F_m dxdydz = 0 \tag{16}$$

and hence for $m \neq n$,

$$\omega_m \neq \omega_n$$

and $\iiint F_m F_n dxdydz = 0$

q.e.d.

APPENDIX B

STANDING WAVES IN MULTIPLY CONNECTED CAVITIES USING A GREEN'S FUNCTION APPROACH

An alternative description of the cavity sound field in terms of its influence or Green's function is sometimes useful. This will be briefly considered here. For further discussion, see Morse and Ingard, Chapter 9, pp. 554-564[6] .

Green's Function Determination

Let $$w(x,y,z) = \delta(x-\xi)\ \delta(y-\eta)\ \delta(z-\zeta)\ e^{i\omega t} \tag{1}$$

Then from II- (7), $$W_n(t) = \frac{1}{A_F}\ F_n(\xi,\eta,\zeta)\ e^{i\omega t} \tag{2}$$

and from II- (8), $$P_n = -\frac{(i\omega)^2\ e^{i\omega t}\ F_n\ (\xi,\eta,\zeta)}{V\ [\omega_n{}^2 - \omega^2]} \tag{3}$$

Thus from II- (9), $$\frac{p}{\rho_o c_o{}^2} = \sum_n \frac{F_n(\xi,\eta,\zeta)F_n(x,y,z)}{M_n[\omega_n{}^2-\omega^2]}\ \frac{[-(i\omega)^2]e^{i\omega t}}{V} \tag{4}$$

The summation

$$-\frac{(i\omega)^2}{V}\ \sum_n \frac{F_n\ (\xi,\eta,\zeta)F_n(x,y,z)}{M_n[\omega_n{}^2 - \omega^2]} \equiv G \tag{5}$$

may be thought of as a Green's function giving the pressure at x, y, z due to a point harmonic displacement of unit amplitude at ξ,η,ζ.

Two Coupled Cavities

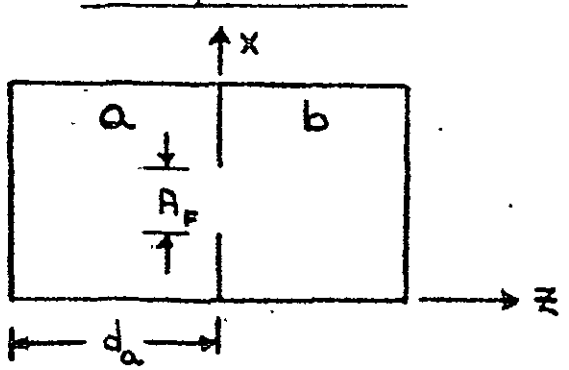

The Green's function may be used to treat two cavities connected by a opening. For definiteness we consider rectangular cavities, although it will be clean the basic

method is applicable to fairly general geometries.

Consider two volumes or cavities with their respective Green's functions and a common "wall area", A_F.

$$G_a = -\frac{(i\omega)^2}{V} \sum_n \frac{F_n^a(\xi,\eta,\zeta)F_n^a(x,y,z)}{M_n^a[\omega_n^{a^2} - \omega^2]} \tag{6}$$

$$G_b = +\frac{(i\omega)^2}{V} \sum_n \frac{F_n^b(\xi,\eta,\zeta)\, F_n^b(x,y,z)}{M_n^b\,[\omega_n^{b^2} - \omega^2]} \tag{7}$$

There is a + sign on G_b because of the sign convention for normal to A_F. Also note that only on A_F do <u>both</u> G_a and G_b apply.

Now

$$\frac{\overline{p}_a}{\rho_o c_o^2}(x,y,z = 0 \text{ on } A_F) = \iint_{\text{over } A_F} G_a(x,y,z = 0 \text{ on } A_F;\xi,\eta,\zeta = 0)\, \overline{w}_a(\xi,\eta,\zeta = 0)\, d\xi d\eta \tag{8}$$

and

$$\frac{\overline{p}_b}{\rho_o c_o^2}(x,y,z = 0 \text{ on } A_F) = \iint_{\text{over } A_F} G_b(x,y,z = 0 \text{ on } A_F;\xi,\eta,\zeta = 0)\, \overline{w}_a(\xi,\eta,\zeta = 0)\, d\xi d\eta \tag{9}$$

Now further we have on A_F, the physical continuity conditions

$$\overline{w} \equiv \overline{w}_a = \overline{w}_b \text{ and } \overline{p}_a = \overline{p}_b \tag{10}$$

Thus using (8) - (10)

$$\iint_{\text{on } A_F} [G_a - G_b]\, \overline{w}\; d\xi d\eta = 0 \tag{11}$$

This is a homogenuous integral equation for w. It is an eigenvalue equation which can be solved in several ways, e.g. collocation method or modal methods, for the coupled cavities natural frequencies.

One may also consider further complications due to the wall in one cavity moving in a prescribed way. For example at $z = -d_a$ in room a, say, $\overline{w} = \overline{w}_a^{\,d}(\xi,\eta)$. Note A_F now includes both walls, $\zeta=0$ and $\zeta = -d_a$. Then

$$\overline{p}_a(x,y,z=0) = \iint_{A_F\,\zeta=0-d_a} G_a(x,y,z=0;\xi,\eta,\zeta=0)\overline{w}_a(\xi,\eta)d\xi d\eta$$

$$+ \iint_{A_F\,\zeta=-d_a} G_a(x,y,z=0;\xi,\eta,\zeta=-d_a)\overline{w}_a^{\,d}(\xi,\eta)d\xi d\eta \qquad (12)$$

and from (9), (10), (12)

$$\iint_{\text{on } A_F\,\zeta=0\;\; z=0} [G_a-G_b]\overline{w}d\xi d\eta + \iint_{\text{on } A_F} G_a(x,y,z=0;\ \xi,\eta,\zeta=-d_a)\overline{w}_a^{\,d}\, d\xi d\eta = 0 \qquad (13)$$

Given $\overline{w}_a^{\,d}$, one may solve for $\overline{w}$ and hence from (8) and (9), determine $\overline{p}$ in both cavities. In particular if $\overline{w}$ and $\overline{w}_a^{\,d}$ are now expanded in terms of structural modes, ψ_m, and one uses (6) and (7) in (11) and (13), (11) becomes (V-12) and (13) becomes (V-15). These same results are derived in a more compact way using the approach of Section V. Hence the present discussion will not be pursued further.

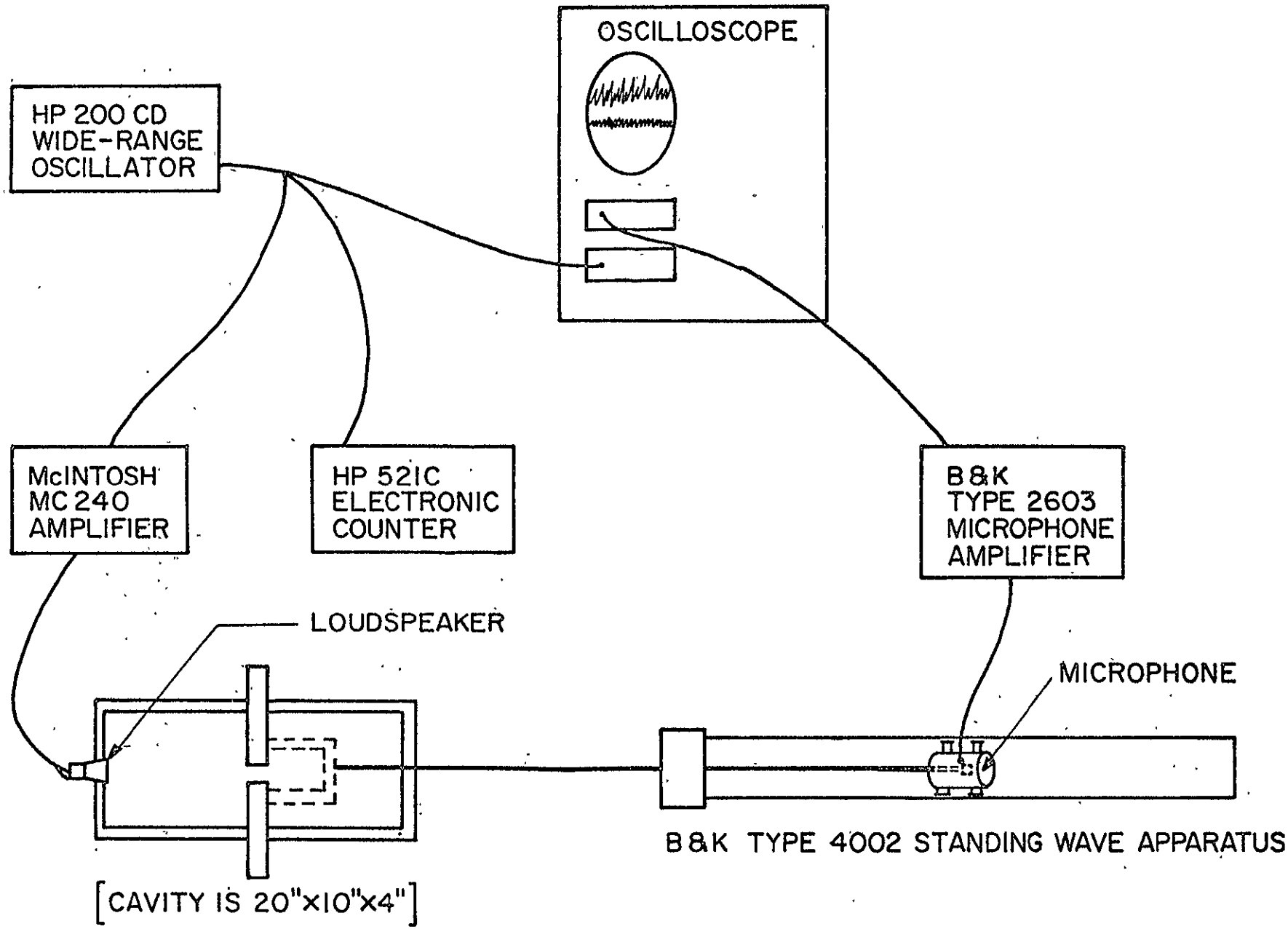

EXPERIMENTAL SET-UP

FIGURE 1

CAVITY NATURAL FREQUENCIES VS. PARTITION SIZE
(2-D CASE, LONGITUDINAL (i.e. X-DIRECTION) MODE)

$$\Omega = \frac{\omega a}{c\pi} = \frac{2af}{c}$$

——— = THEORETICAL RESULTS
ΔΔΔ = EXPERIMENTAL RESULTS

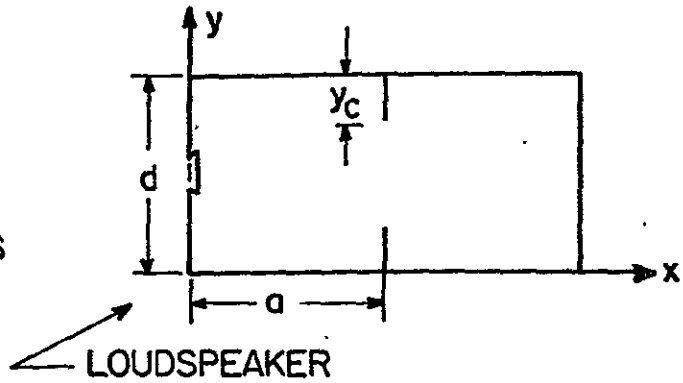

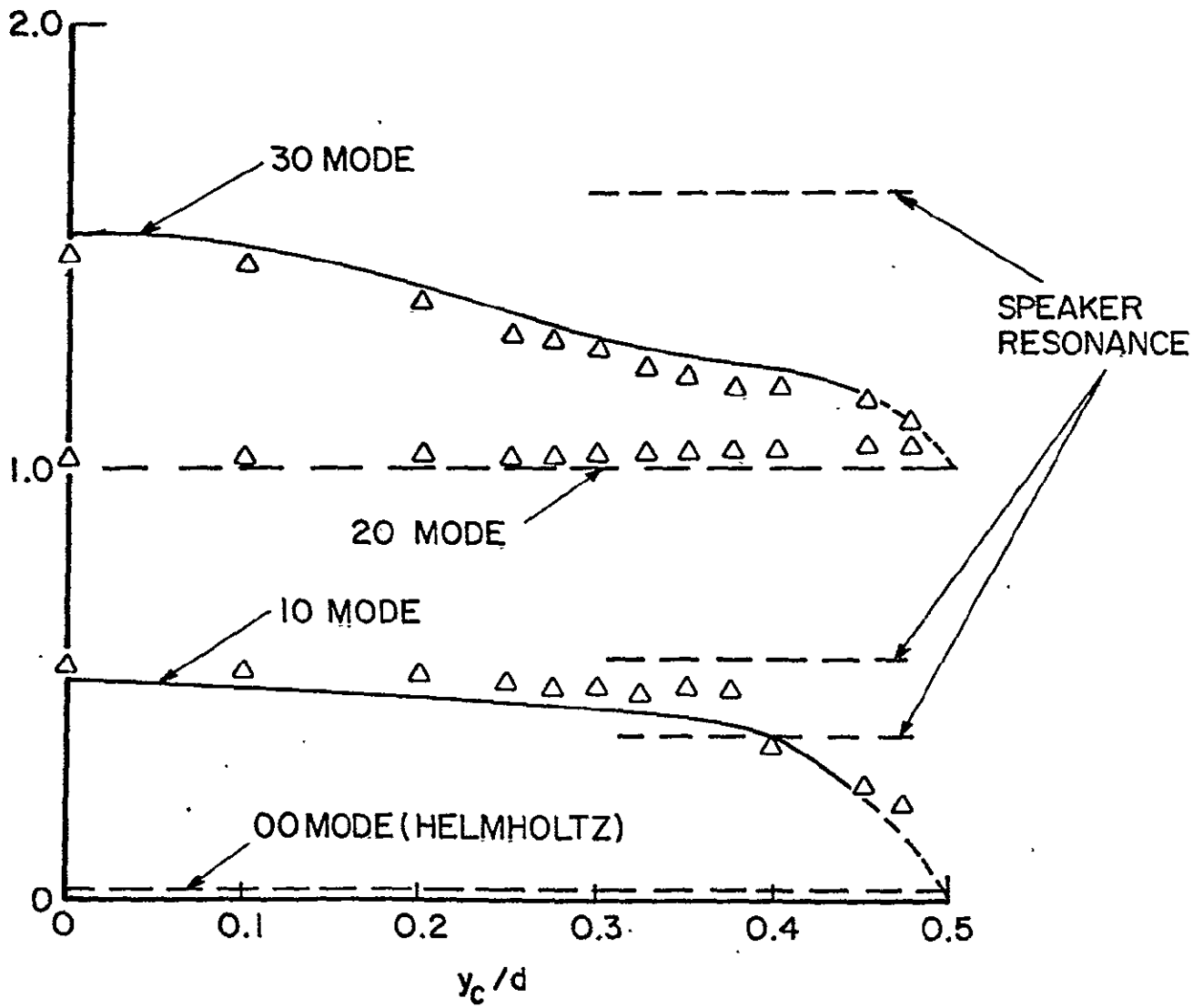

FIGURE 2

NATURAL CAVITY FREQUENCY VS. APERATURE LOCATION
(2-D CASE, LONGITUDINAL (i.e. X-DIRECTION) MODE)

$$\Omega = \frac{\omega a}{c\pi} = \frac{2af}{c}$$

$y_0/d = 0.5$

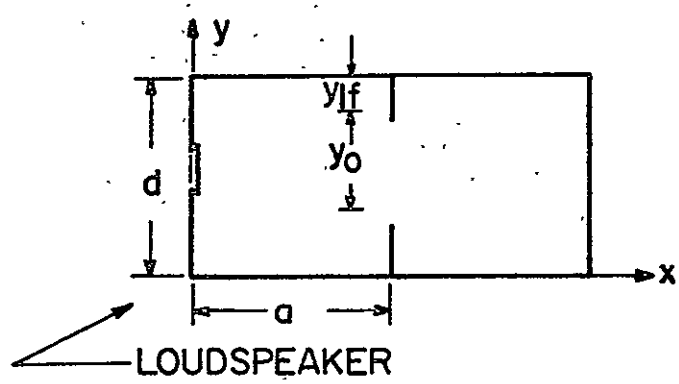

——— = THEORETICAL RESULTS
ΔΔΔ = EXPERIMENTAL RESULTS

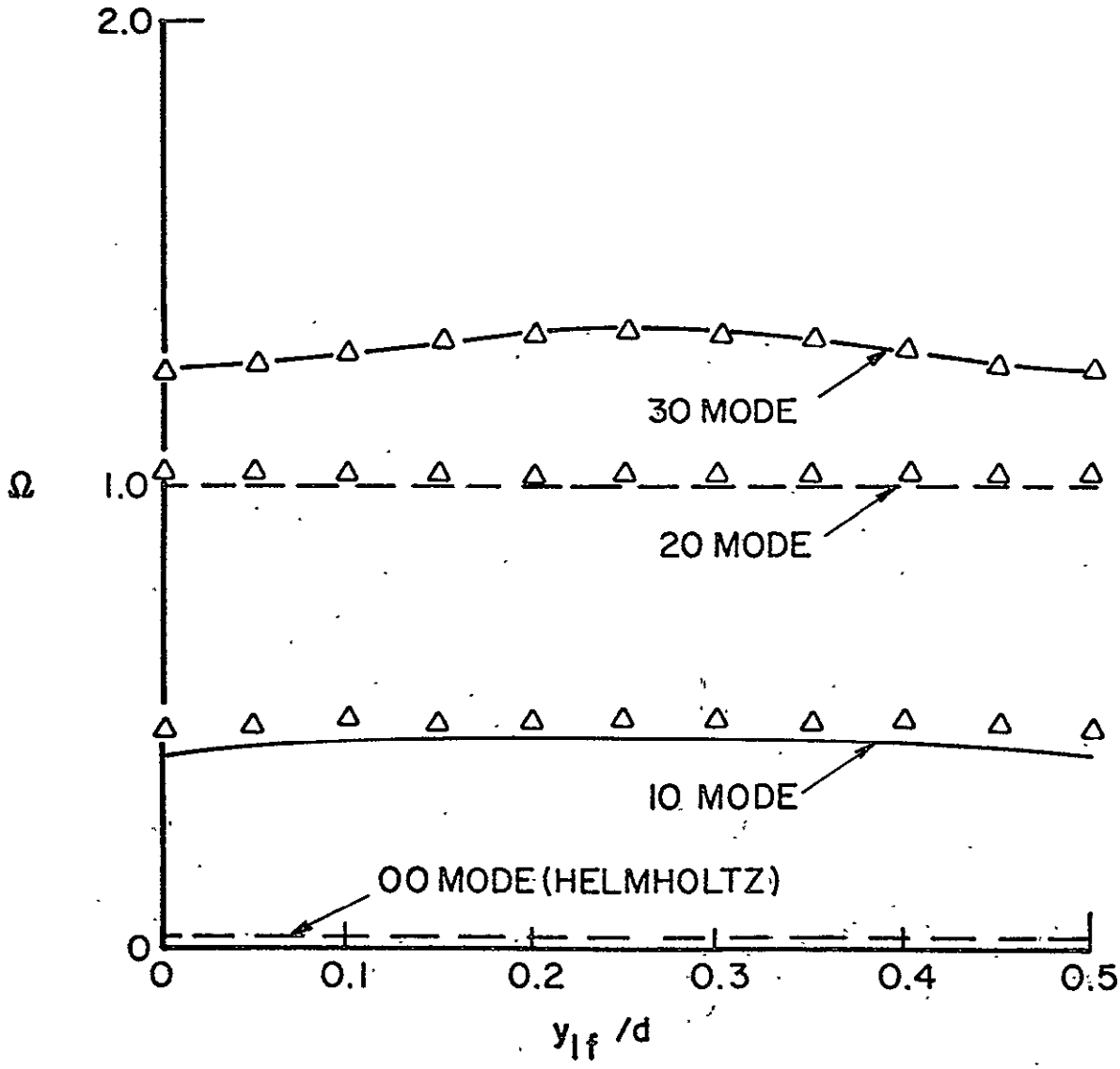

FIGURE 3

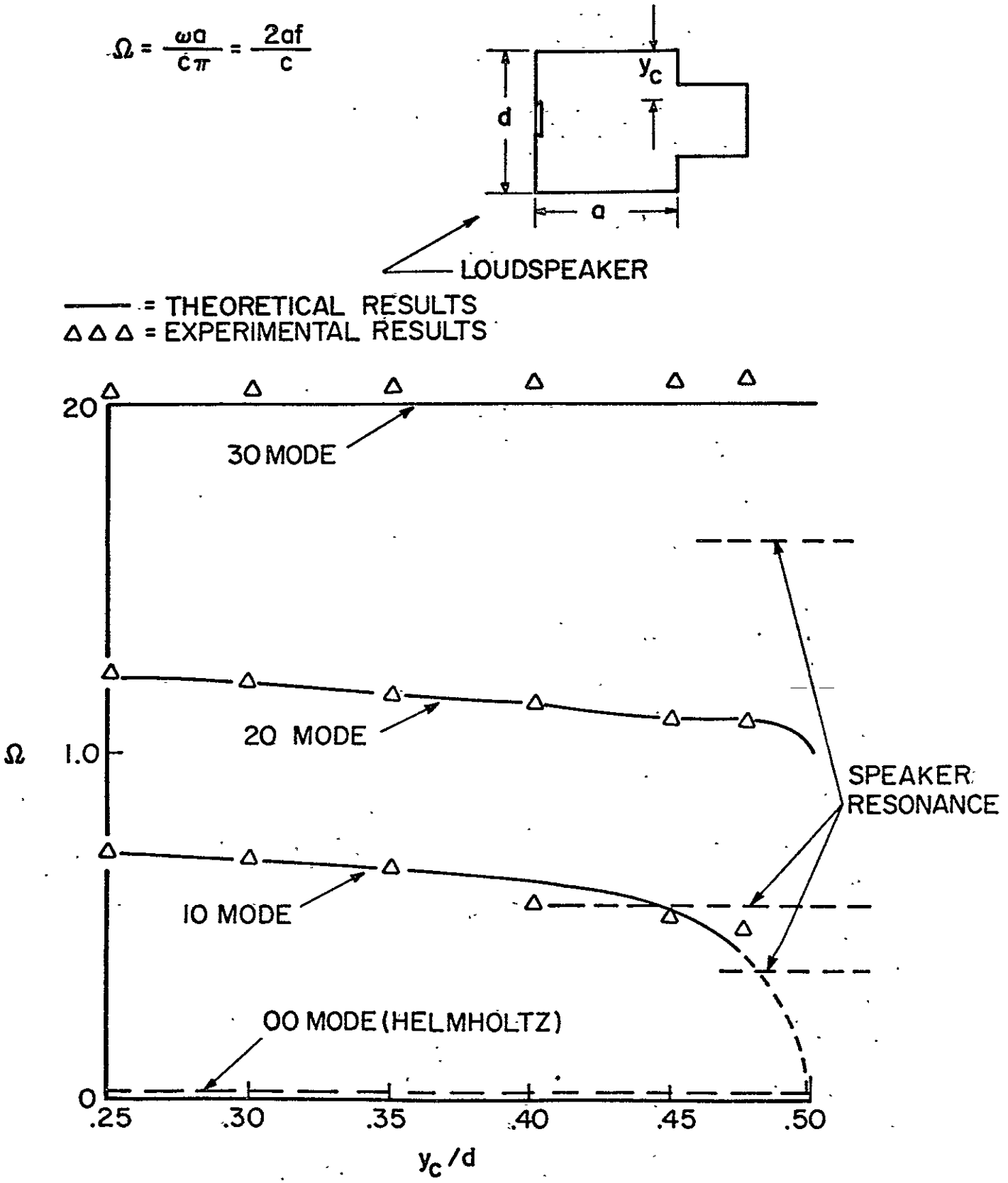

CAVITY NATURAL FREQUENCY VS. PARTITION SIZE
(2-D CASE, LONGITUDINAL MODES)

FIGURE 4

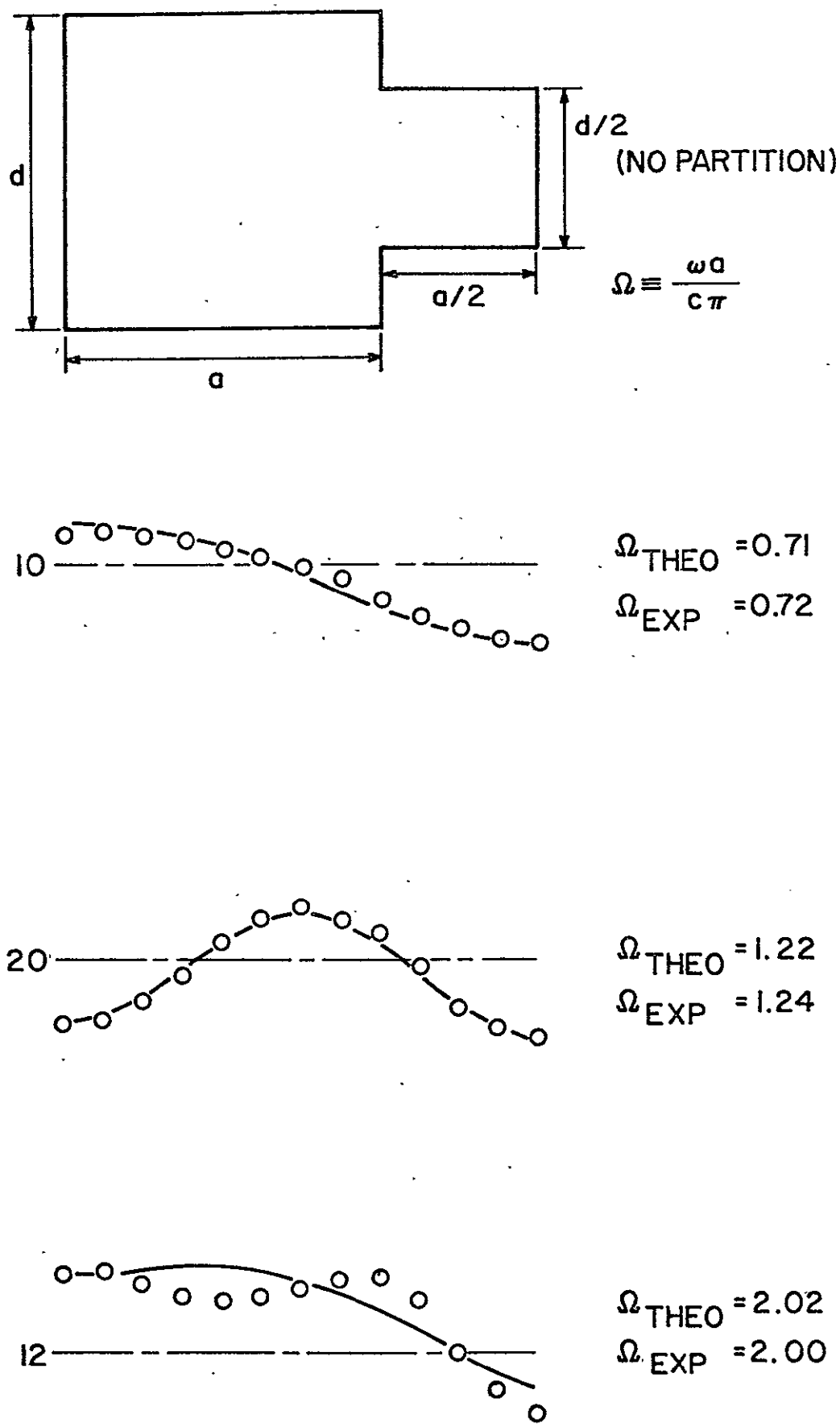
d
d/2
(NO PARTITION)
a/2
a
$\Omega \equiv \frac{\omega a}{c\pi}$
10
Ω_{THEO} =0.71
Ω_{EXP} =0.72
20
Ω_{THEO} =1.22
Ω_{EXP} =1.24
12
Ω_{THEO} =2.02
Ω_{EXP} =2.00

FIGURE 5

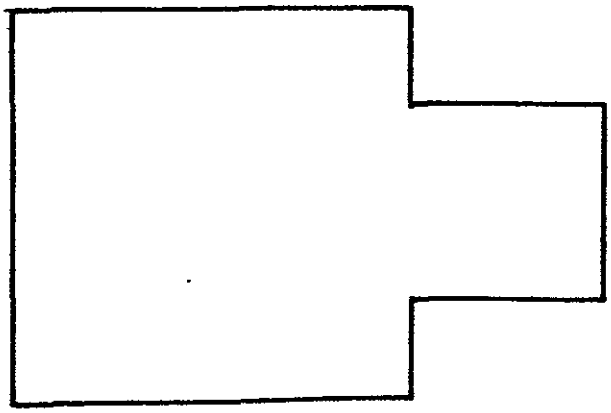

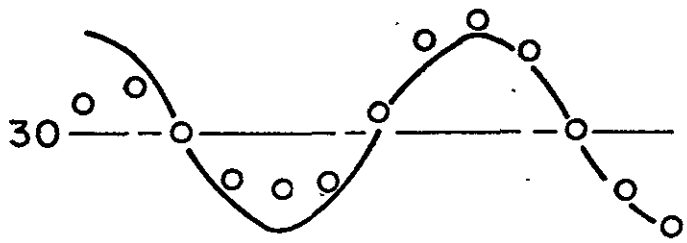

Ω_{THEO} = 2.00
Ω_{EXP} =2.04

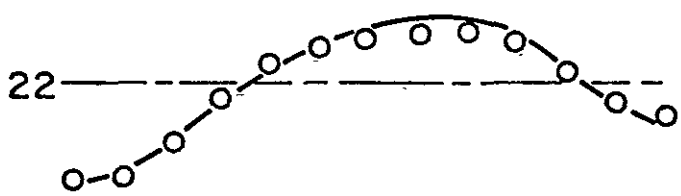

Ω_{THEO} =2.23
Ω_{EXP} =2.23

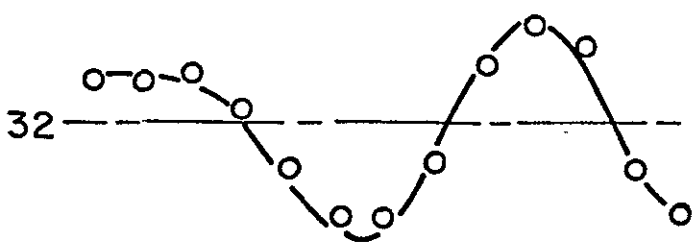

Ω_{THEO} =2.65
Ω_{EXP} =2.62

FIGURE 5 Continued

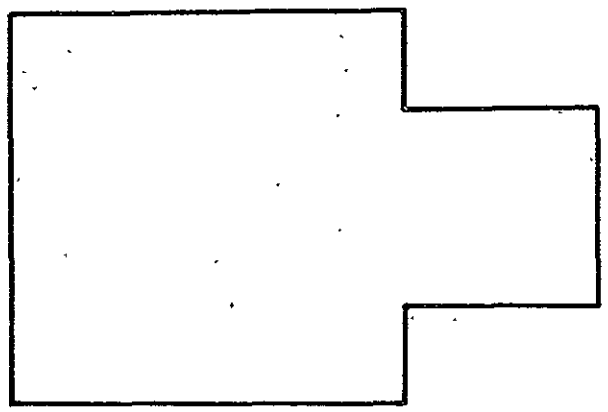

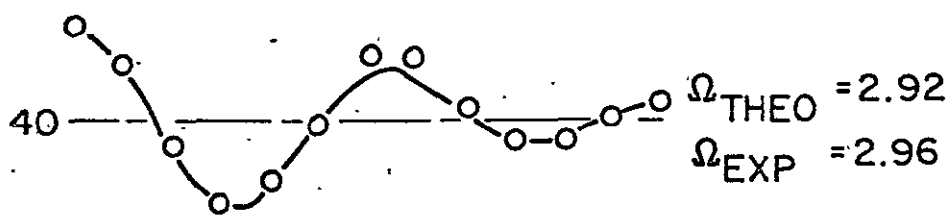

FIGURE 5 Continued

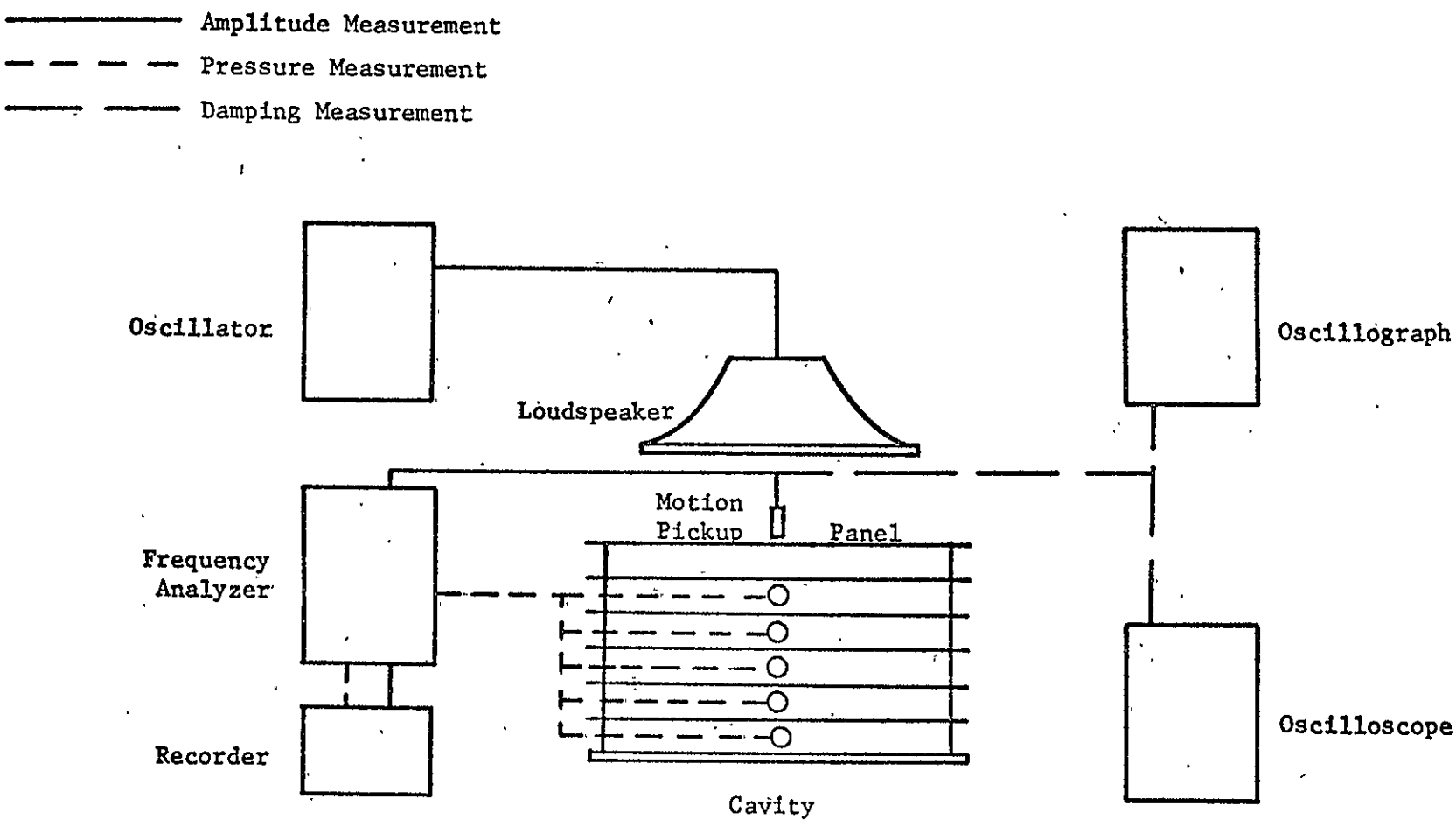

EXPERIMENTAL ARRANGEMENT

FIGURE 6

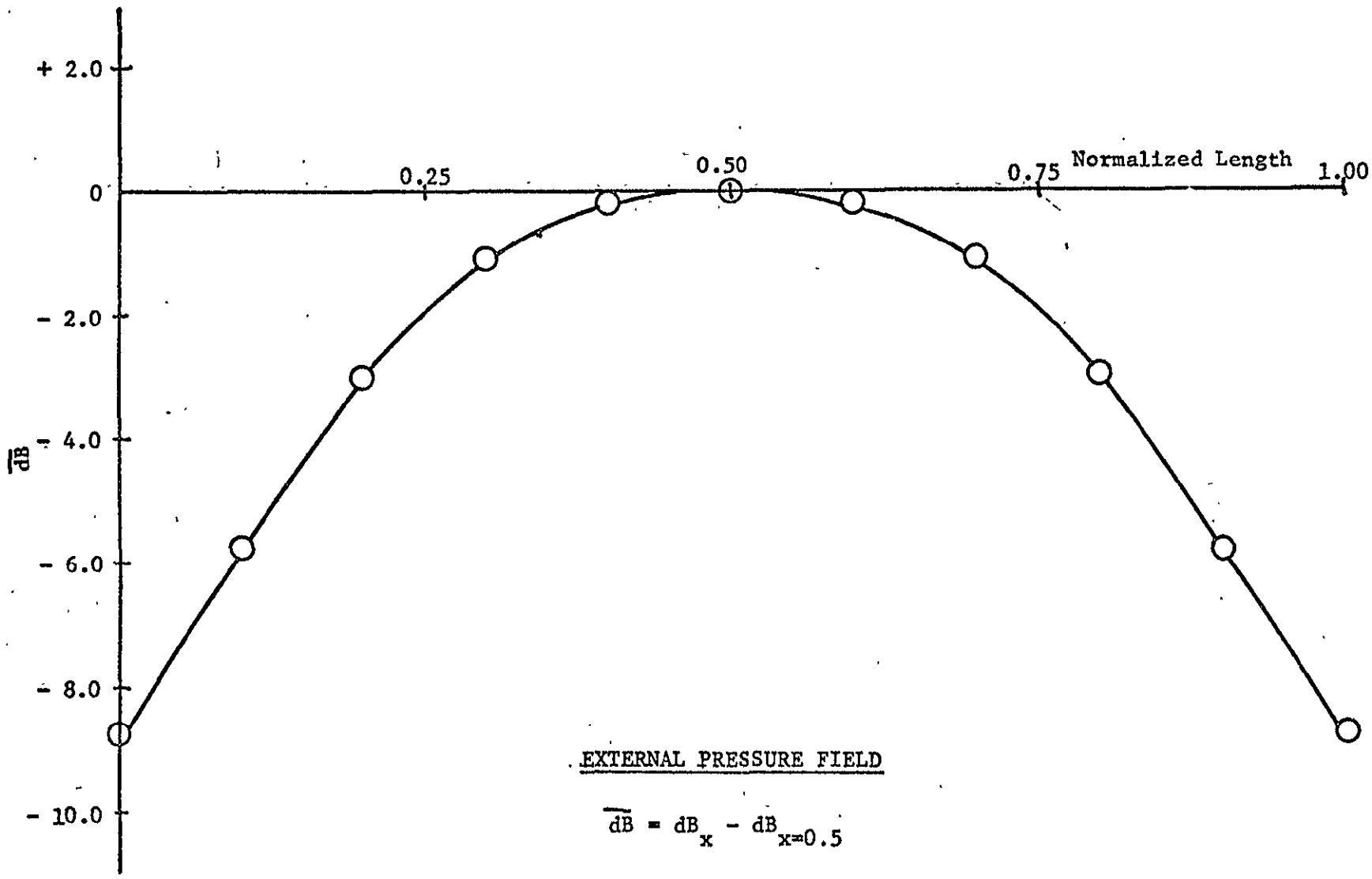
+ 2.0
0
- 2.0
- 4.0
- 6.0
- 8.0
- 10.0
$\overline{dB}$
0.25
0.50
0.75
1.00
Normalized Length
EXTERNAL PRESSURE FIELD
$\overline{dB} = dB_x - dB_{x=0.5}$

FIGURE 7

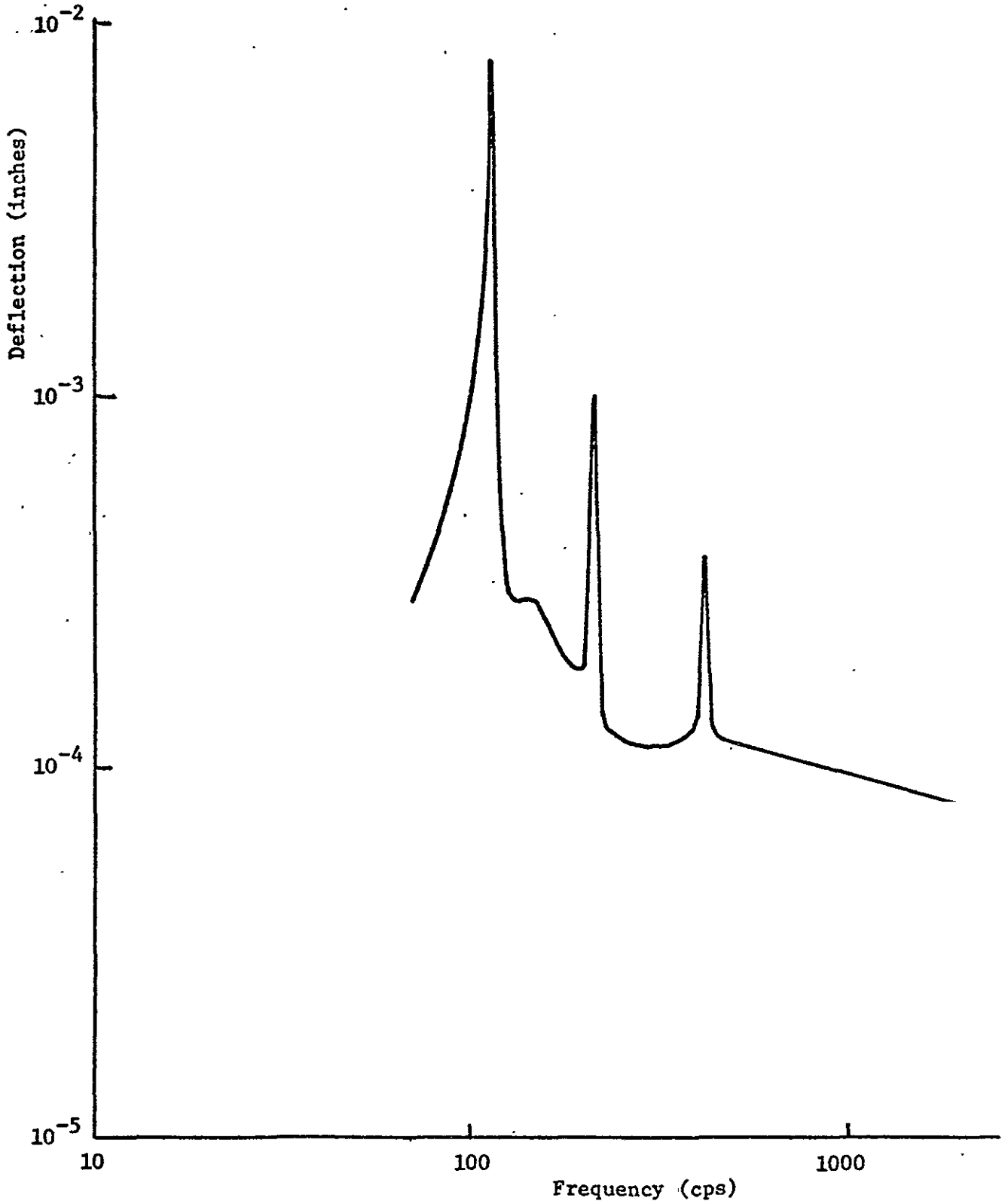

PANEL RESPONSE TO SINUSOIDAL EXTERNAL FIELD

FIGURE 8

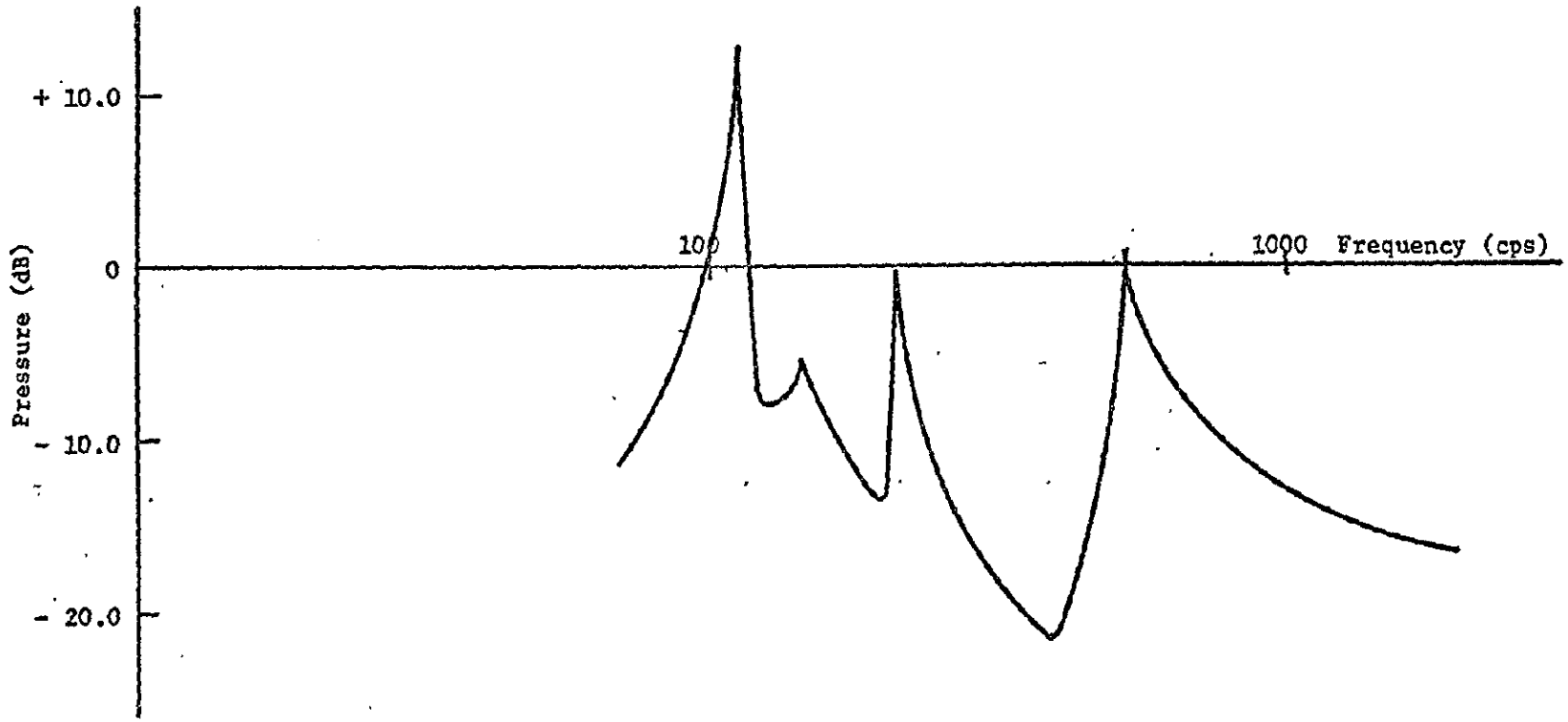

CAVITY RESPONSE TO SINUSOIDAL EXTERNAL FIELD

FIGURE 9

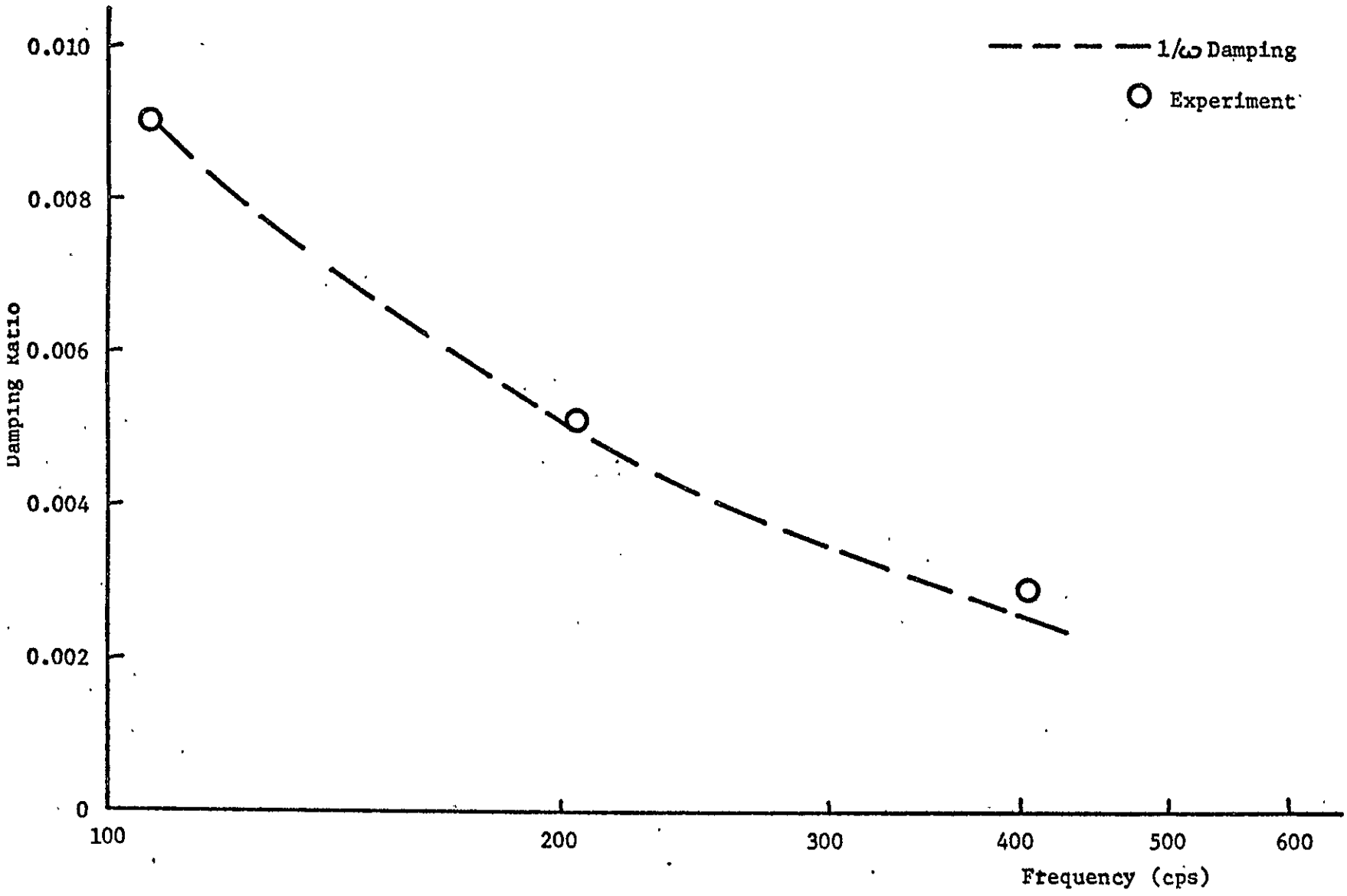

PANEL DAMPING VS. FREQUENCY

FIGURE 10

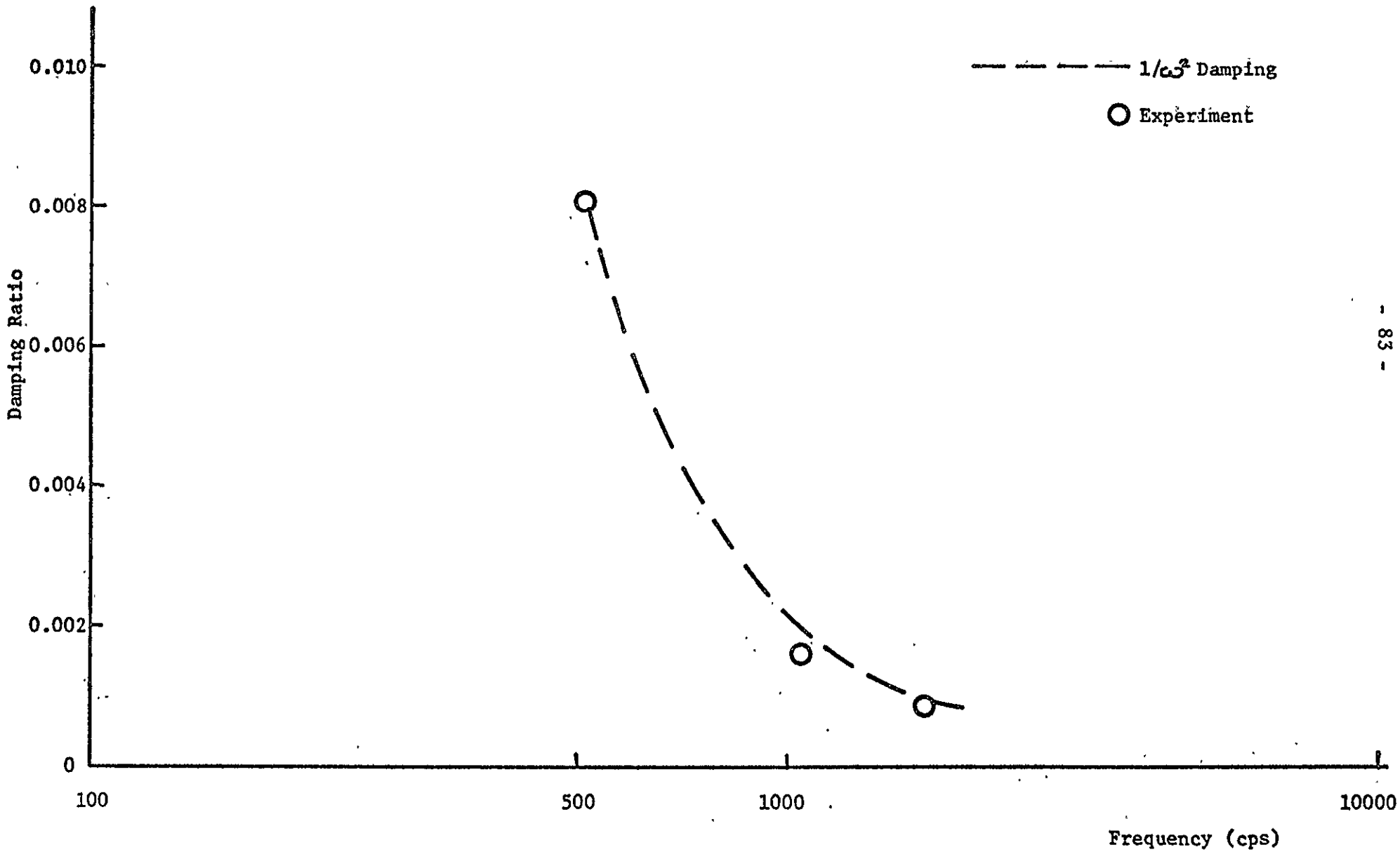

CAVITY DAMPING VS. FREQUENCY

FIGURE 11

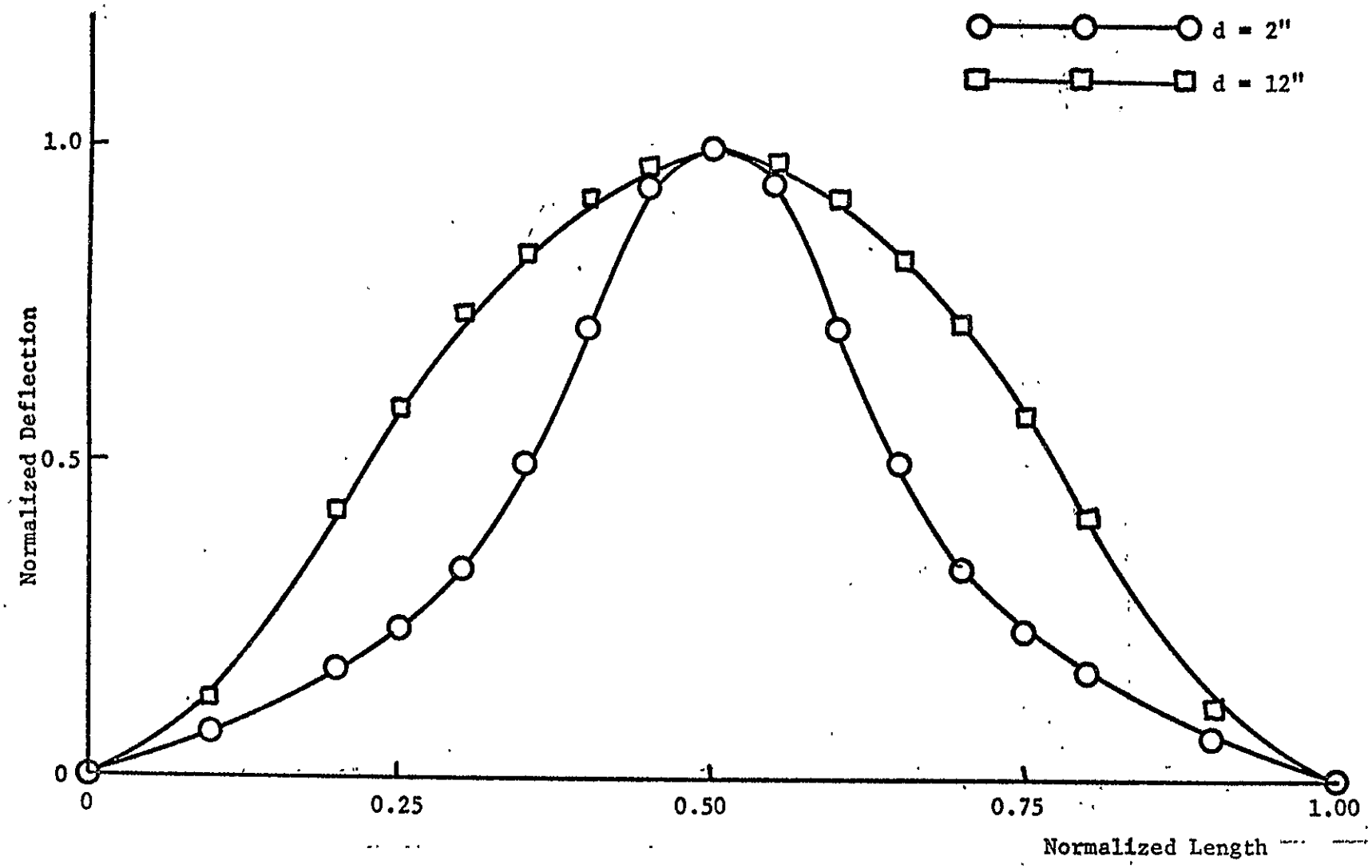

CAVITY EFFECT ON PANEL NORMAL MODE SHAPES
(Fundamental Mode)
FIGURE 12

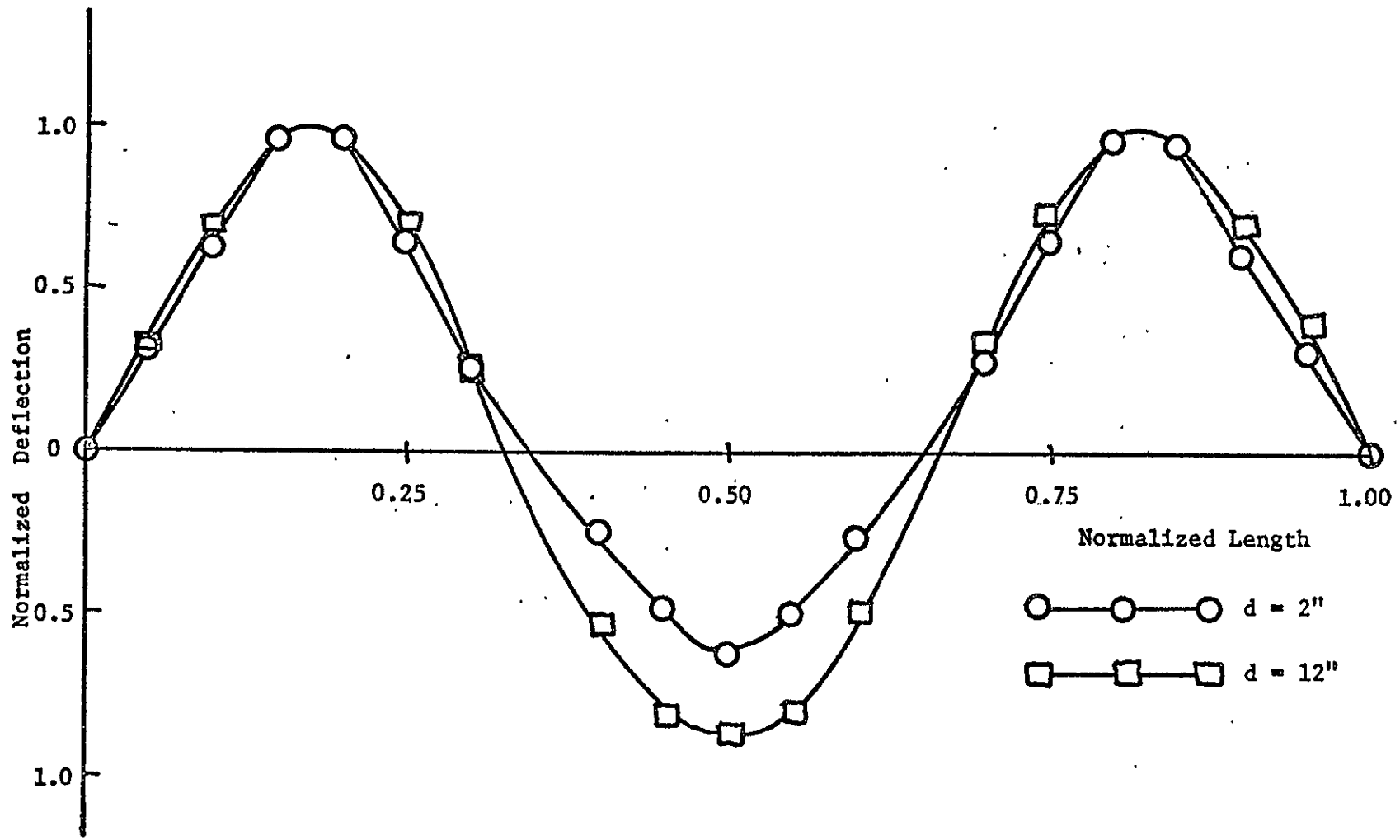

CAVITY EFFECT ON PANEL NORMAL MODE SHAPES
(Third Mode)
FIGURE 13

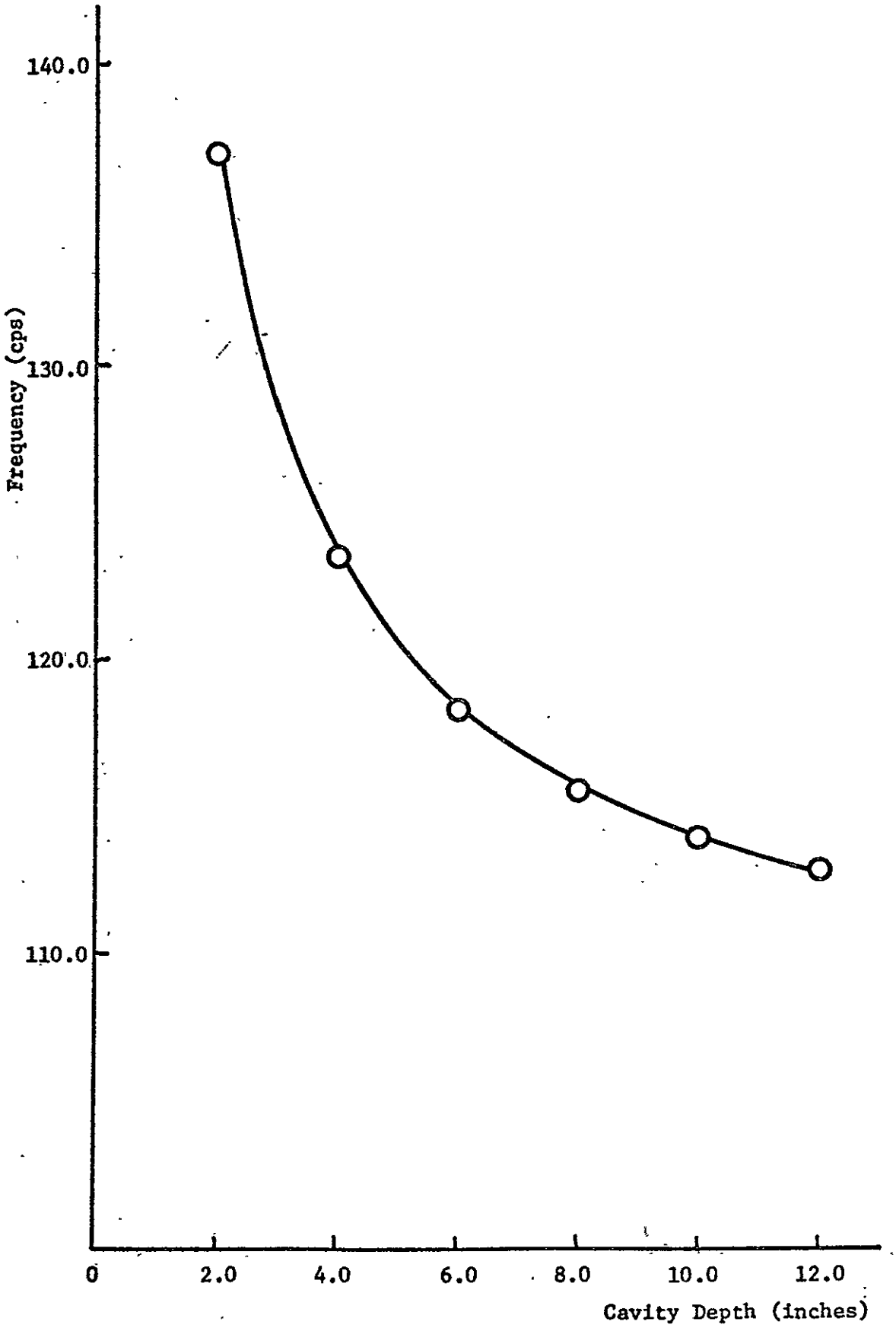

FUNDAMENTAL PANEL FREQUENCY VS. CAVITY DEPTH

FIGURE 14

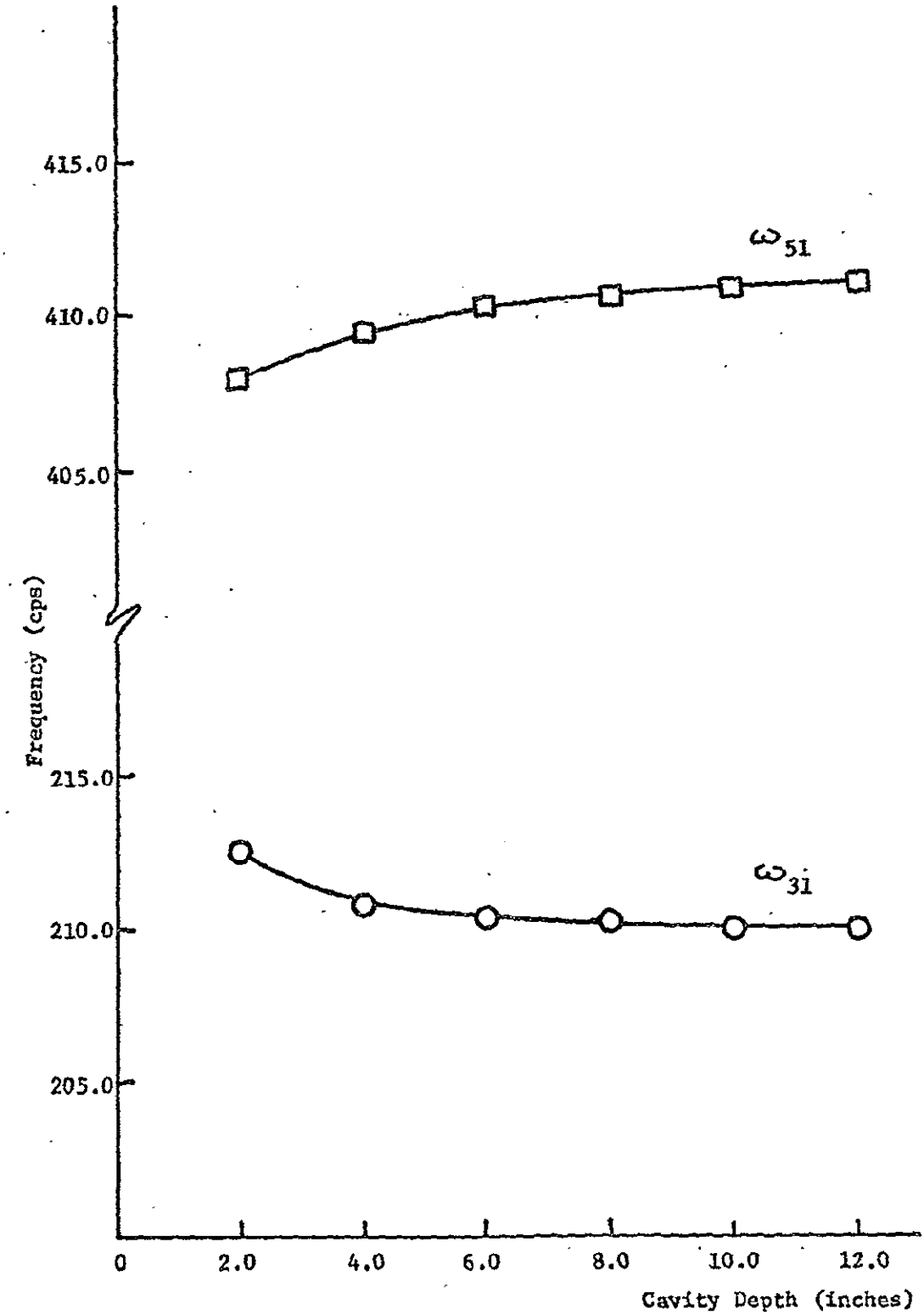

THIRD AND FIFTH PANEL FREQUENCY VS. CAVITY DEPTH

FIGURE 15

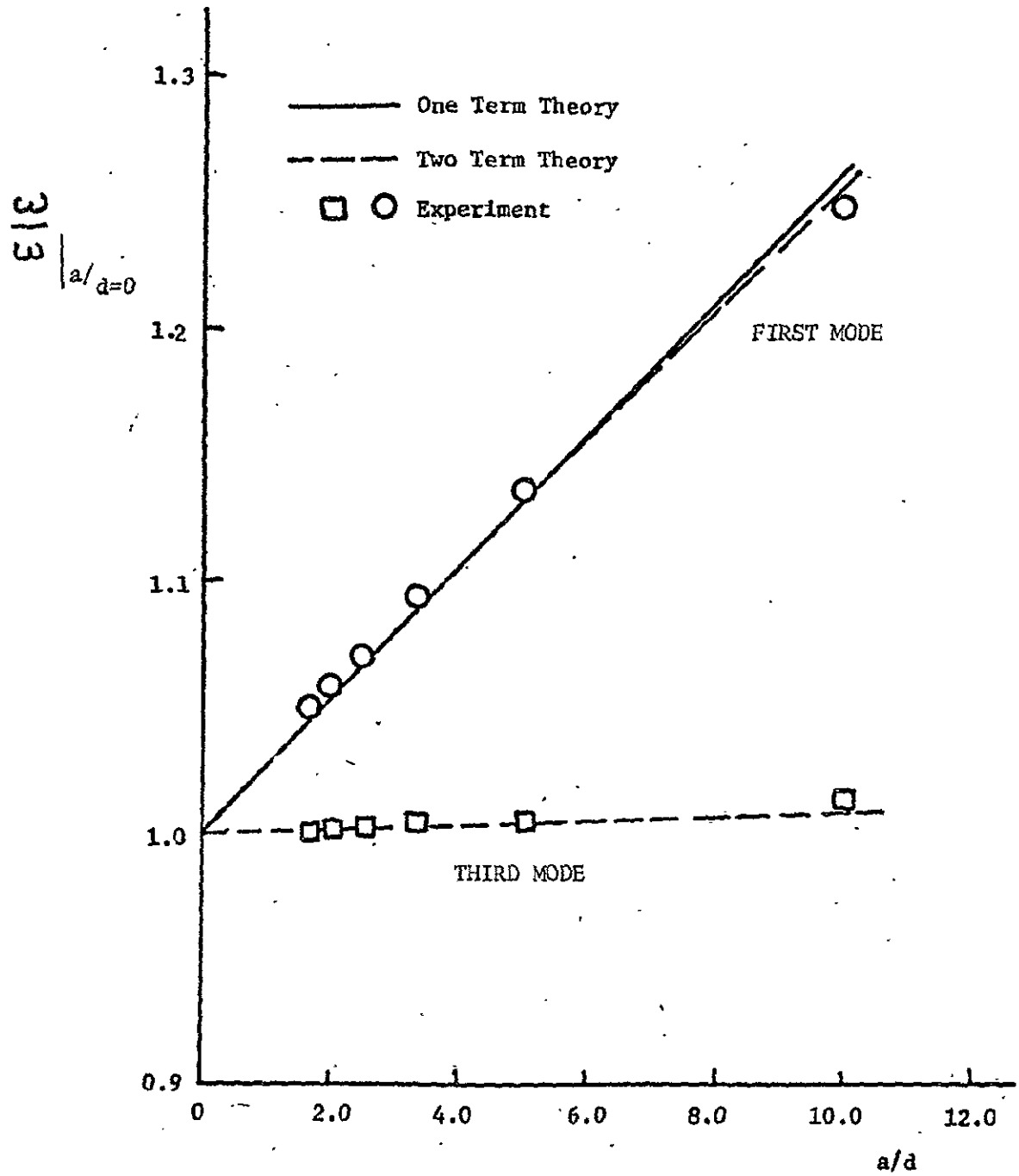

CAVITY EFFECT ON PANEL NATURAL FREQUENCIES

FIGURE 16

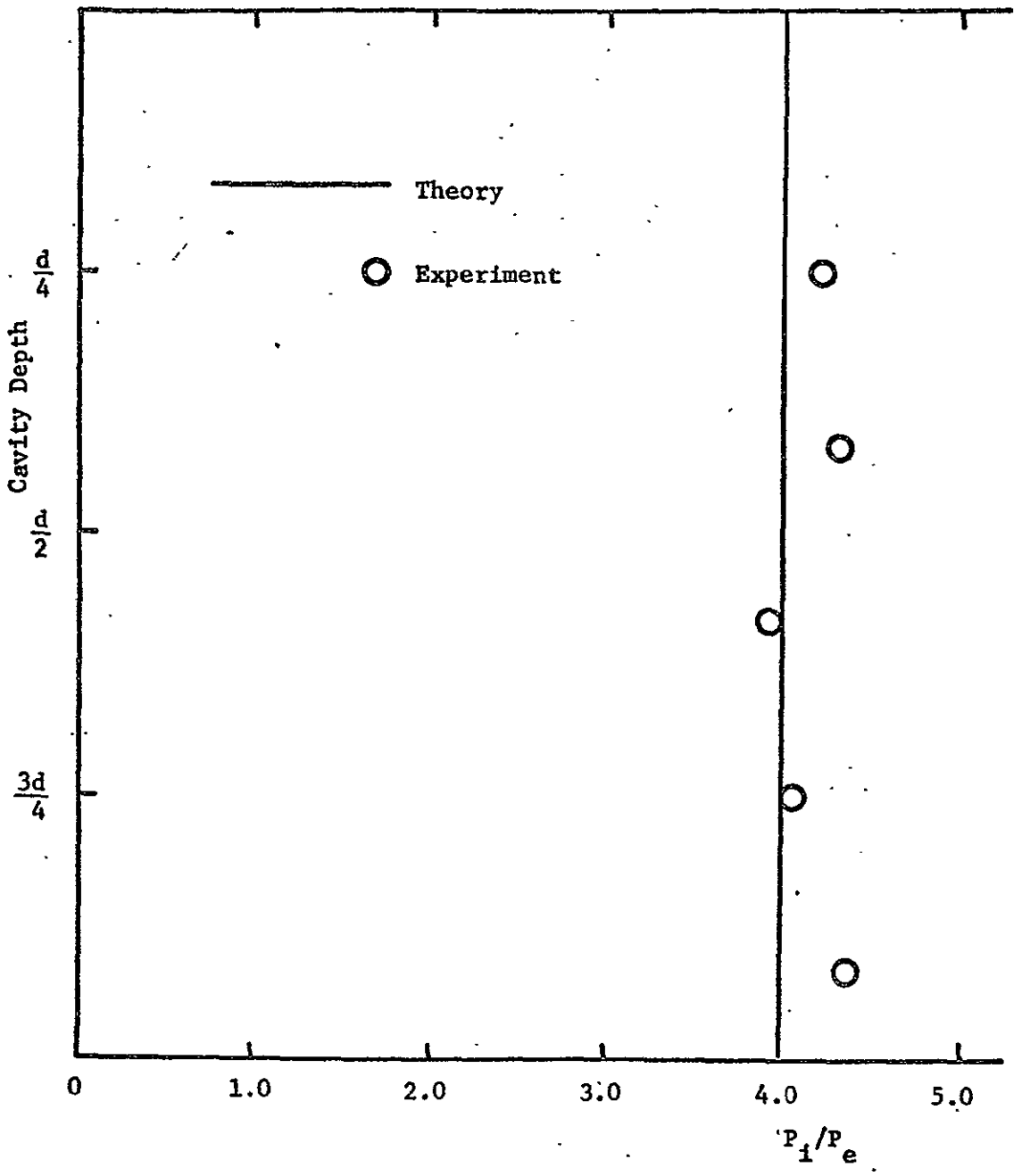

PRESSURE DISTRIBUTION
(at panel fundamental)

FIGURE 17

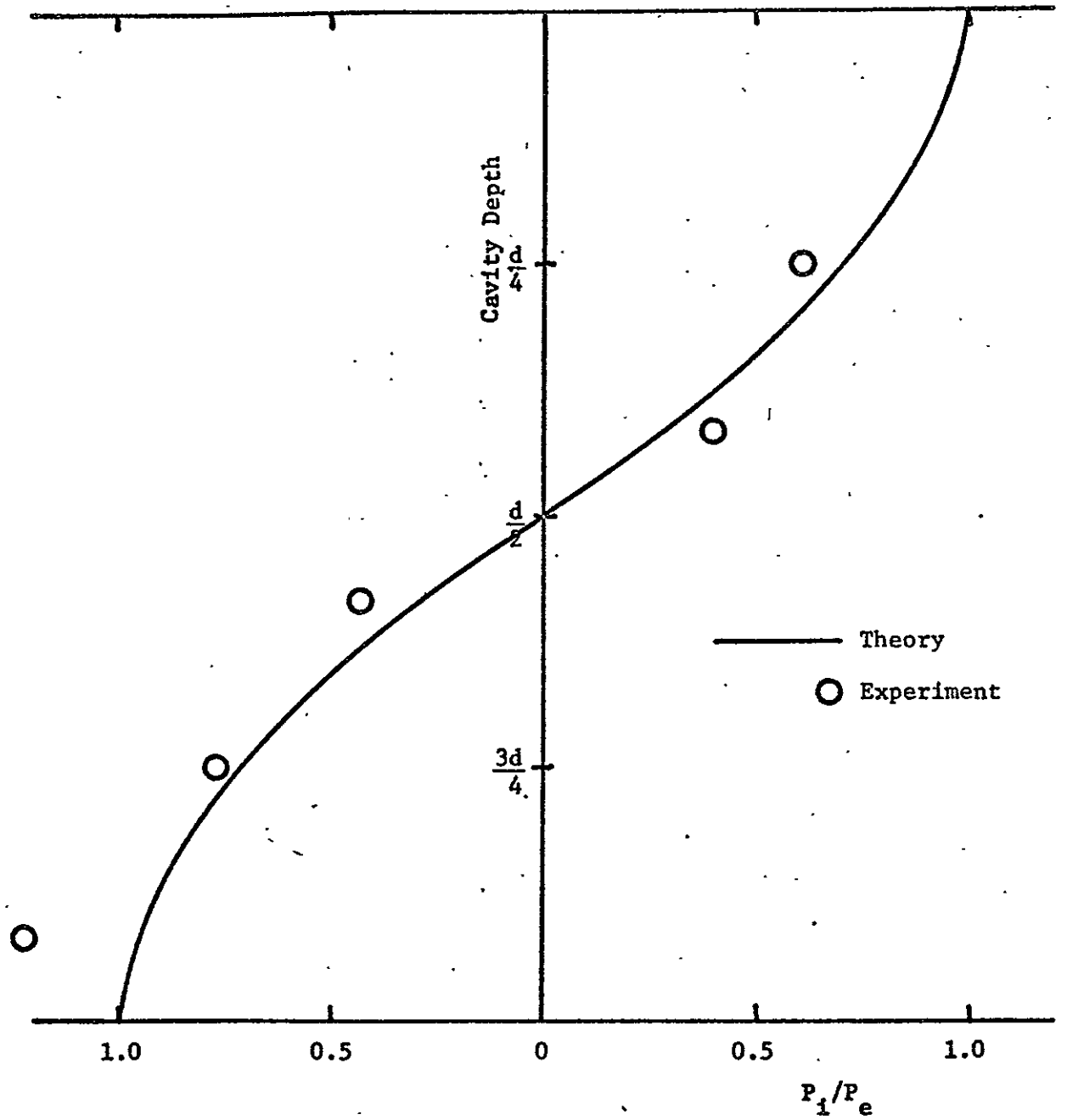

PRESSURE DISTRIBUTION

(at cavity fundamental)

FIGURE 18

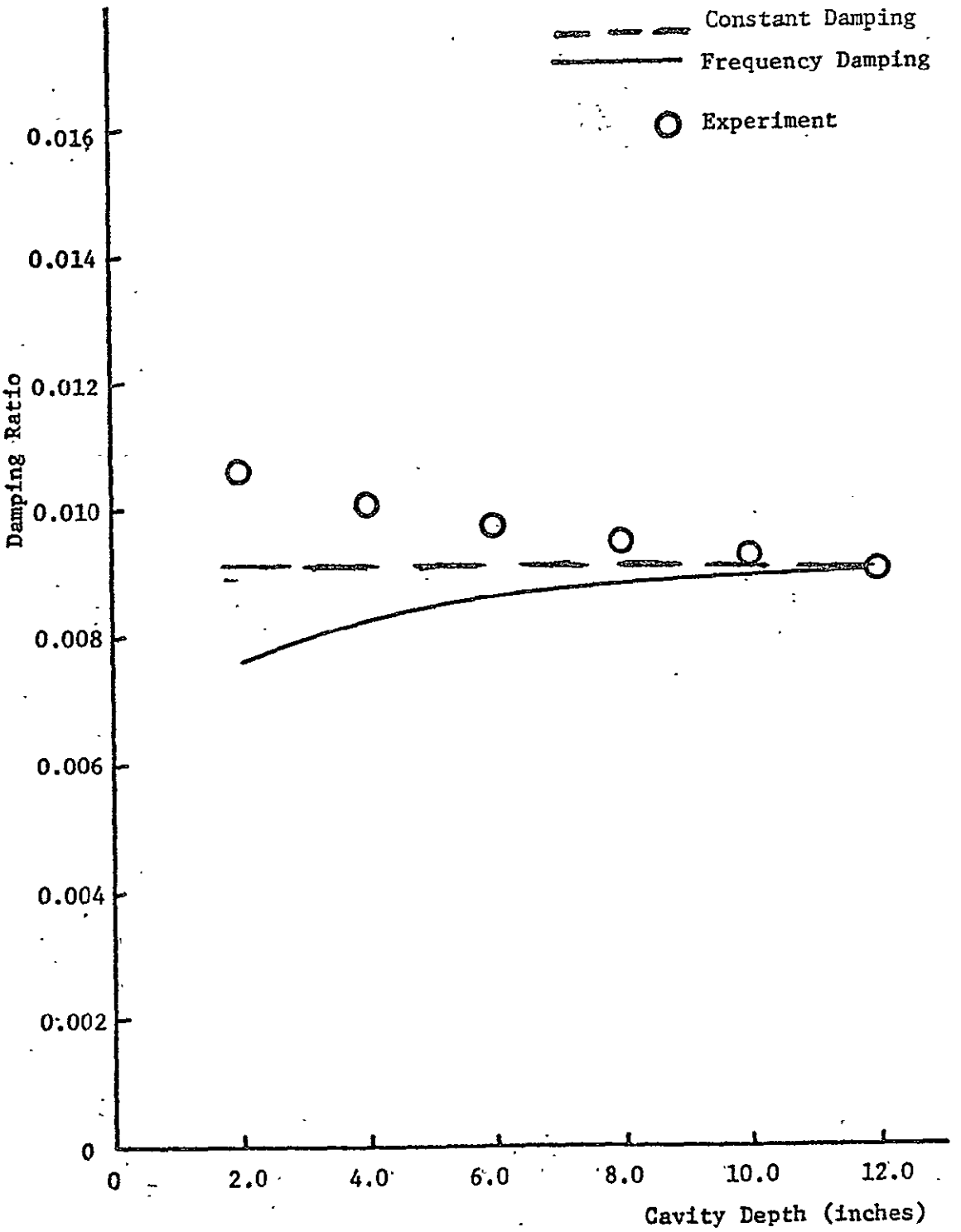

PANEL DAMPING RATIO VS. CAVITY DEPTH

(Panel Fundamental Mode)

FIGURE 19

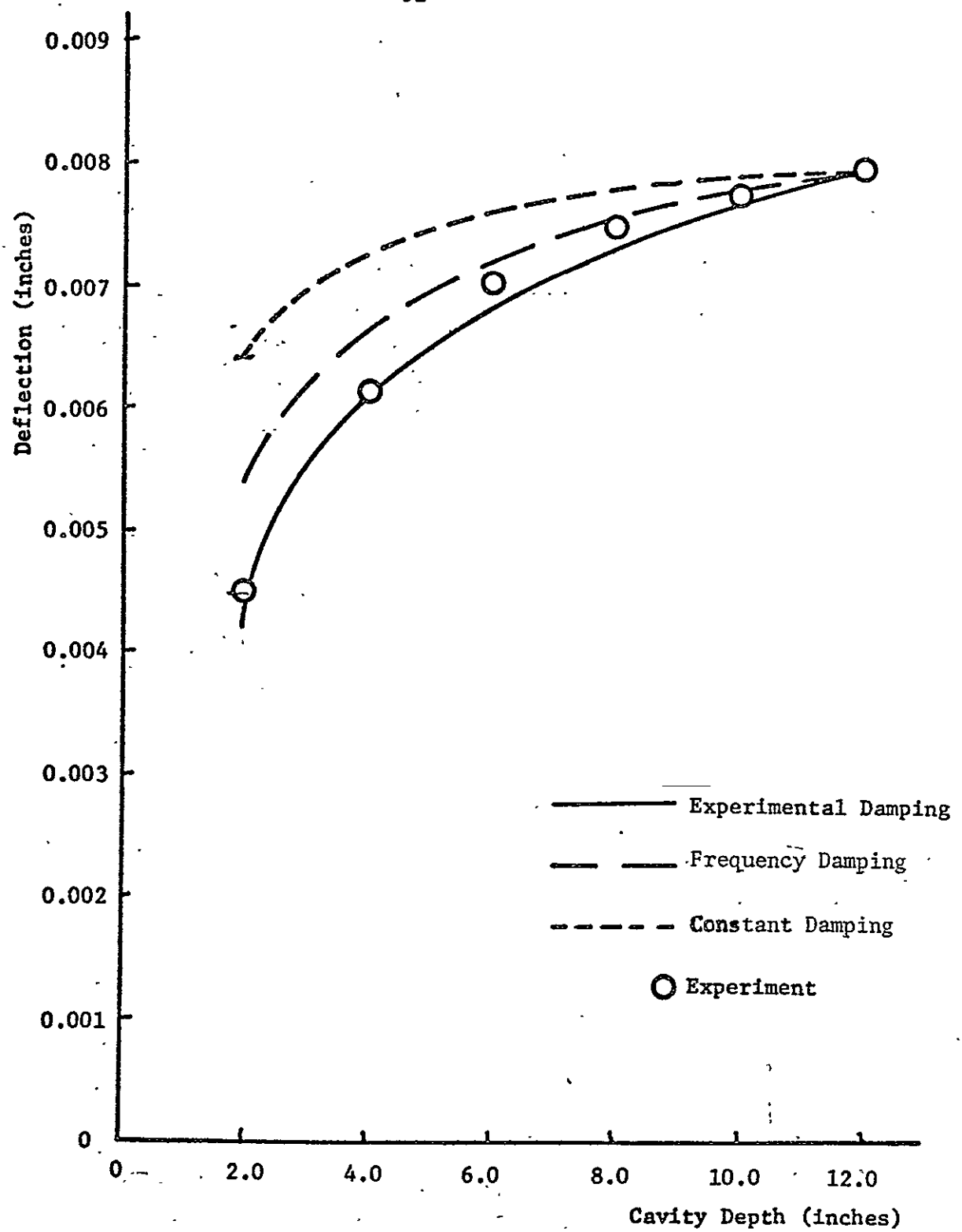

PANEL DEFLECTION VS. CAVITY DEPTH

(Panel Fundamental Mode)

FIGURE 20

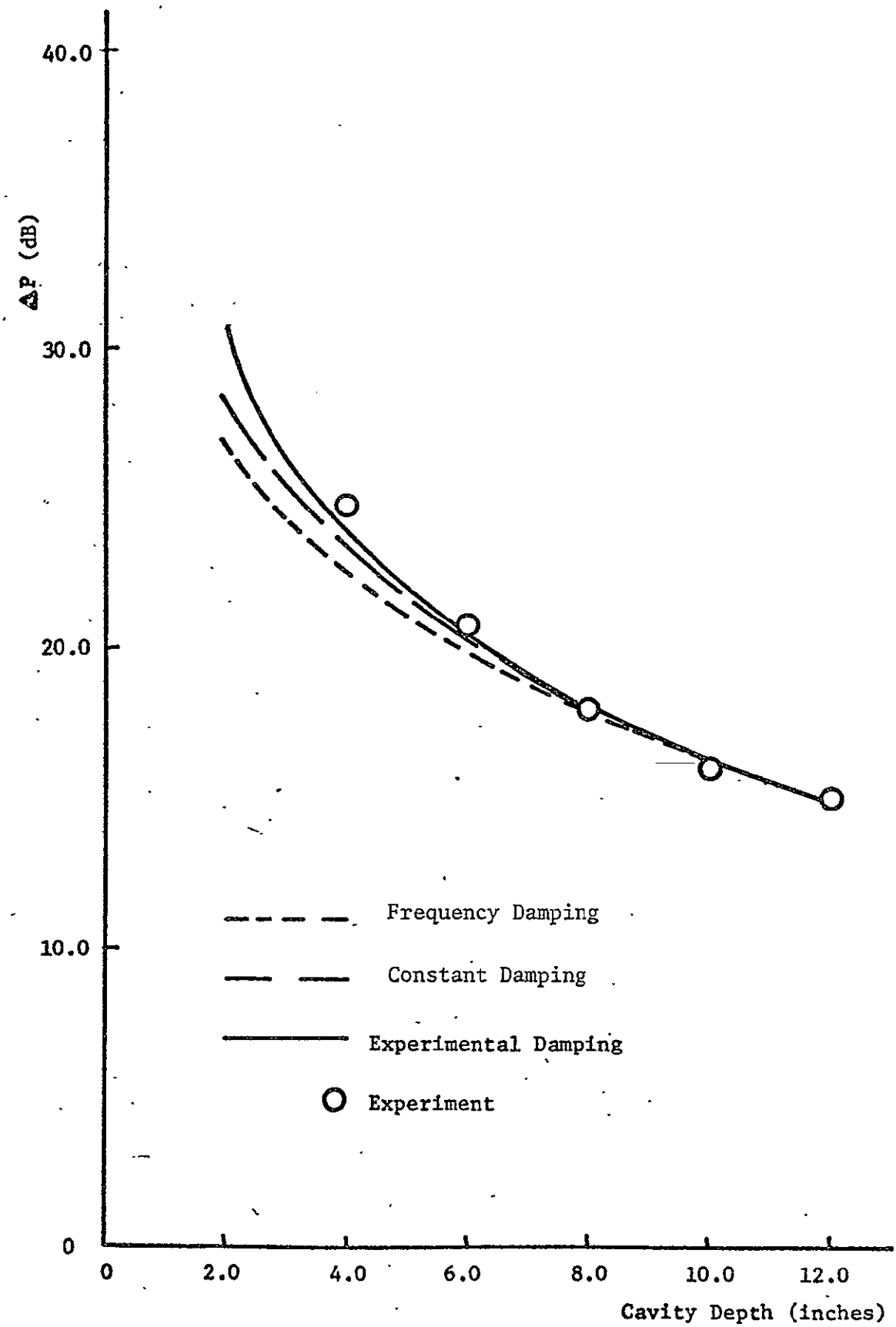

CAVITY PRESSURE VS. CAVITY DEPTH

FIGURE 21